

# Resonances in Atomic and Molecular Physics (and Nuclear!)

Chris Greene, Purdue University

This talk represents one theorist's point of view. But **CAUTION**: not all theorists look at resonances the same way!

For instance, in this talk we will consider resonances **ONLY** from the point of view of remaining on the real energy axis in our analysis of scattering properties.

Other concepts utilized and discussed here that are less commonly covered in theoretical treatments of scattering theory include the following:

- Inclusion of “unphysical” or “closed” channels in the scattering matrix or the reaction matrix
- The time delay matrix of Wigner and Smith for extracting partial widths and for computing the density of states associated with interactions
- Qualitative and Semi-quantitative analysis of collisional resonance physics by interpreting effective potential energy curves

# Outline

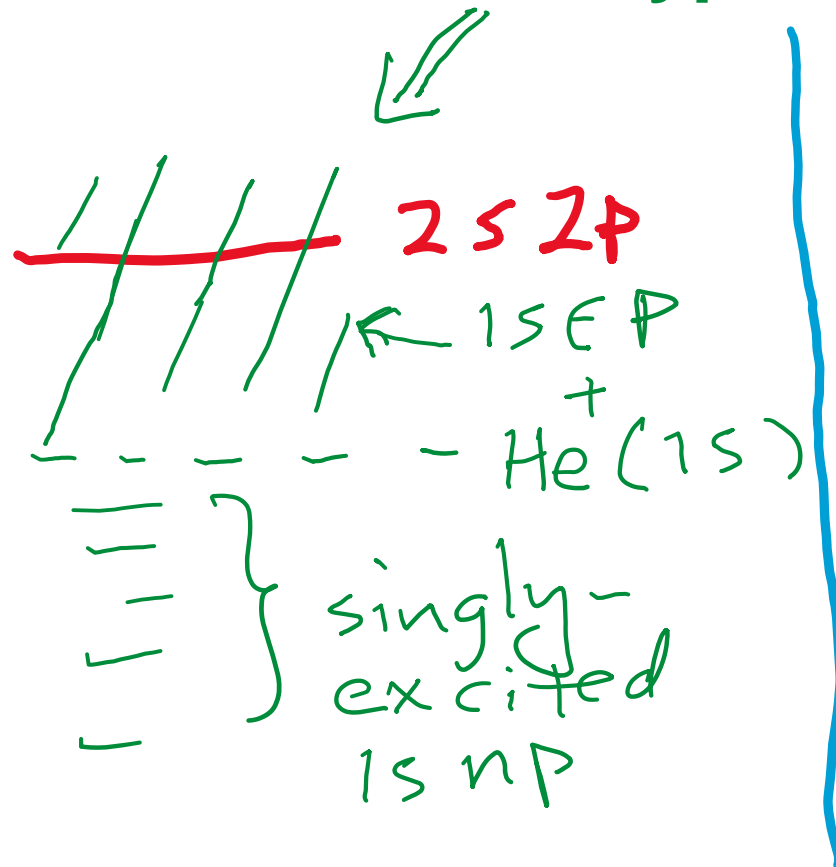
- 1. Basic Fano line shape ideas (in both energy and time)**
- 2. Example of a complex Rydberg spectrum**
- 3. Systematic treatment via MQDT**
  - A) Rydberg systems**
  - B) Ultracold atom-atom collisions**
- 4. Extensions of collision theory beyond 2-body entrance & exit channels: hyperspherical coordinates and potentials**
- 5. Efimov physics and implications for 3 and more particles**

# Topic 1. Basic Fano resonance physics, u.

Fano, Phys. Rev. 124, 1866(1961) ← a citation classic!

The Fano model treats one bound state embedded in one continuum

Prototype system: He doubly-excited states



zeroth-order basis

continuum  $|E\rangle$  obeys

$$\langle E|H|E'\rangle = E'\delta(E-E')$$

bound state obeys

$$\langle \phi|H|\phi\rangle = E_\phi$$

coupling matrix element is:

$$\langle \phi|H|E\rangle = V_E \quad (\text{and } \langle \phi|E\rangle = 0)$$

Then a stationary state solution is a linear combination,

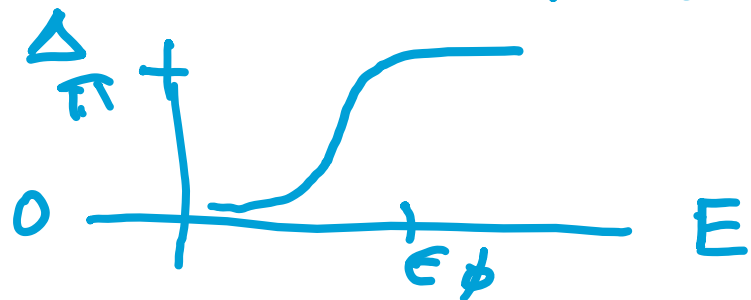
$$|\Psi_E\rangle = |\phi\rangle a(E) + \int d\epsilon |\epsilon\rangle b_\epsilon(E)$$

Solution  $|\Psi_E\rangle = a(E) \left\{ |\phi\rangle + |\epsilon\rangle \pi \eta(E) + \int d\epsilon' |\epsilon'\rangle \frac{\mathcal{P}}{E - \epsilon'} V_{\epsilon'} \right\}$

$$\eta(E) = -\cot \Delta = \left( \frac{\pi |V_E|^2}{E - \epsilon_\phi - E} \right)^{-1}$$

Here  $\Delta$  appears as an  $E$ -dependent phaseshift in the perturbed continuum state, i.e.

$$\langle \vec{r} | \Psi_E \rangle \xrightarrow{r \rightarrow \infty} \frac{\Phi}{\text{core}} \sin[kr + \delta_0 + \Delta(E)]$$



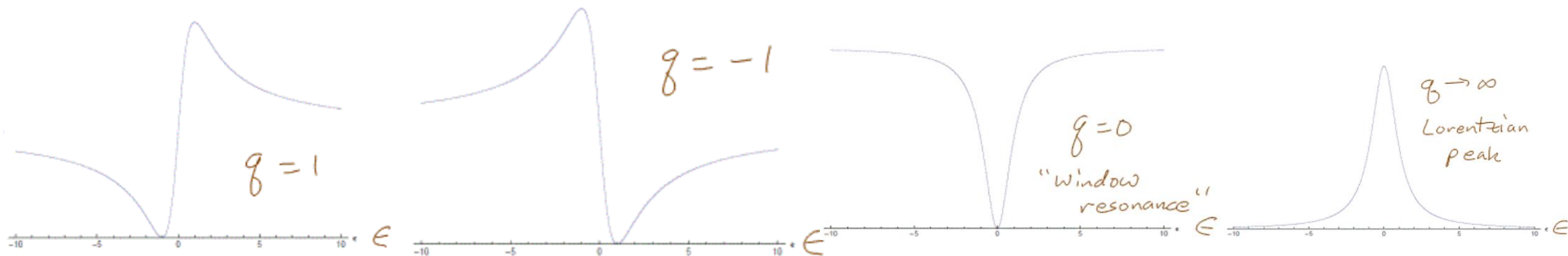
← phaseshift rises by  $\pi$  as  $E$  increases over the resonance

And any observable involving a transition operator  $T$  can exhibit an asymmetric "Fano Lineshape"

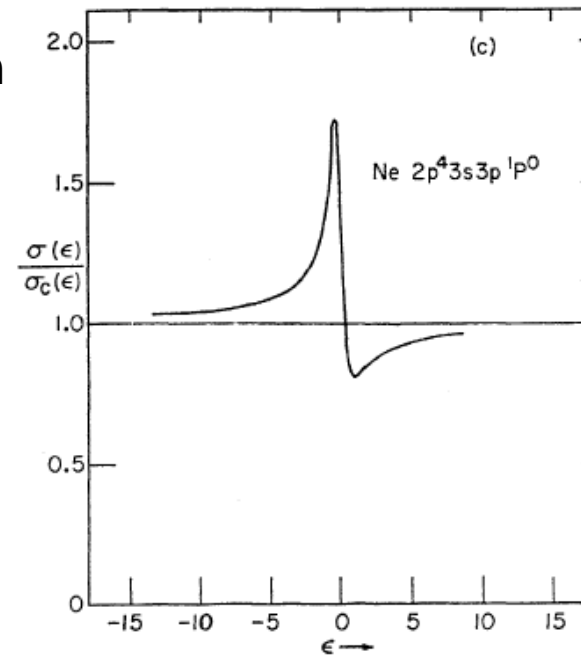
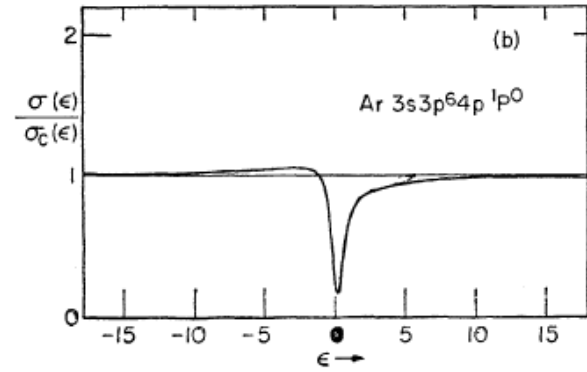
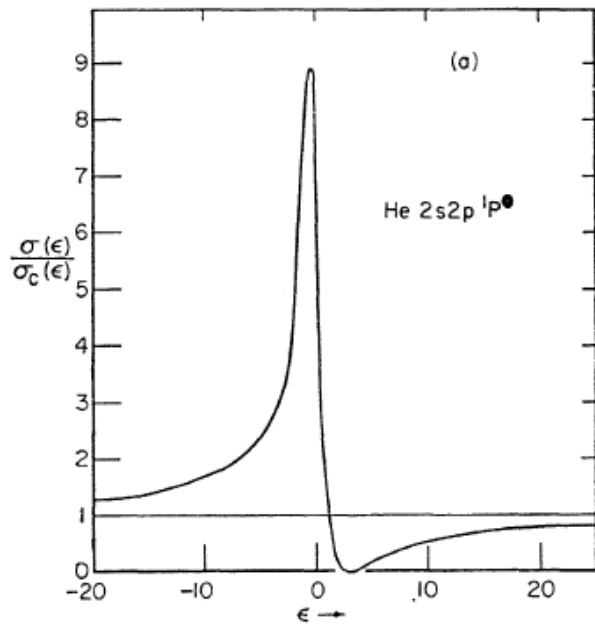
$$\text{i.e. } |\langle \Psi_E | T | i \rangle|^2 = |\langle \epsilon | T | i \rangle|^2 \frac{\left[ q + \frac{E - E_{res}}{\Gamma/2} \right]^2}{1 + \left( \frac{E - E_{res}}{\Gamma/2} \right)^2}$$

$$q = \frac{\langle \Phi | T | i \rangle}{\pi V_E^* \langle \epsilon | T | i \rangle}$$

Fano lineshape  
 $q$ -parameter  
 controls asymmetry



## Examples of different Fano lineshapes in rare gas atom photoionization



From Fano & Cooper,  
1968 Rev. Mod. Phys.

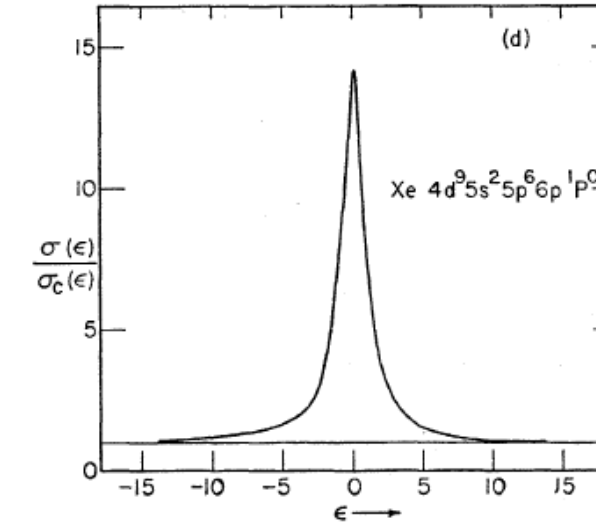


FIG. 27. Profiles of autoionization lines in the rare gases obtained from experimental data (MC65, CME67, CME68, Ed67). (a)  $2s2p\ ^1P^0$  in He ( $q = -2.8$ ,  $\rho^2 = 1$ ); (b) Inner subshell excitation in Ar,  $3s3p64p\ ^1P^0$  ( $q = -0.22$ ,  $\rho^2 = 0.86$ ); (c) Two-electron excitation in Ne,  $2p^4(^3P)3s3p\ ^1P^0$  ( $q = -2.0$ ,  $\rho^2 = 0.17$ ). (d) Inner shell excitation in Xe,  $4d^9 5s^2 5p^6 6p\ ^1P^0$  ( $q \sim 200$ ,  $\rho^2 \sim 0.0003$ ).

Note that the occurrence of non-Lorentzian lineshapes is very common in AMO phenomena, as in the first 3 examples above.

A more recent development:

Implications of a Fano resonance for time domain phenomena

Reference: C. Ott, et al., Science 340, 716 (2013)

Idea: The photoionization formula at a Fano resonance gives the imaginary part of the dielectric constant, and a Kramers-Kronig treatment then gives the real part by computing a principal value integral, namely

$$\operatorname{Re} \frac{\epsilon(\omega)}{\epsilon_0} = 1 + \frac{1}{\pi} \mathcal{P} \int_{-\infty}^{\infty} \frac{\operatorname{Im} \frac{\epsilon(\omega')}{\epsilon_0}}{\omega' - \omega} d\omega'$$

Now imagine an ultrafast laser that is essentially a delta function in time, exciting this resonance. It will initiate an electric dipole response that decays (with the autoionization lifetime) and oscillates with a phase, which is determined by the Fano lineshape  $q$  parameter:

$$\tilde{d}(t) \propto \delta(t) + \frac{\Gamma}{2} e^{-\Gamma t/2} (q-i)^2 e^{-i\omega_{fi}t}$$

The factor  $(g-i)^2$  can be written as an amplitude and a phase factor, i.e.

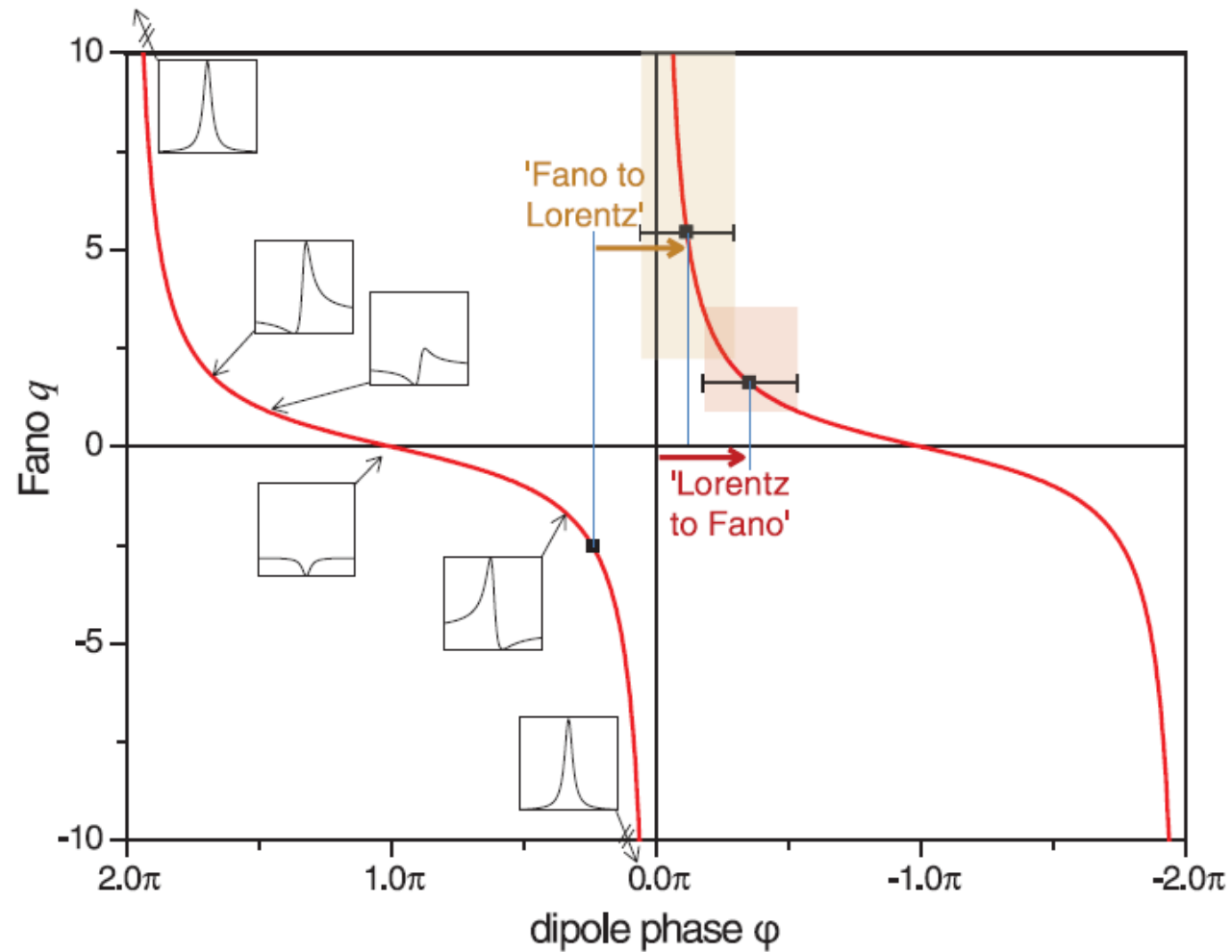
$$(g-i)^2 = (g^2+1)e^{i\phi(g)}$$

where  $\phi(g) = -2 \cot^{-1}(g)$

This result has been verified by the O'H, Pfeifer et al. experiment presented in the 2013 Science article



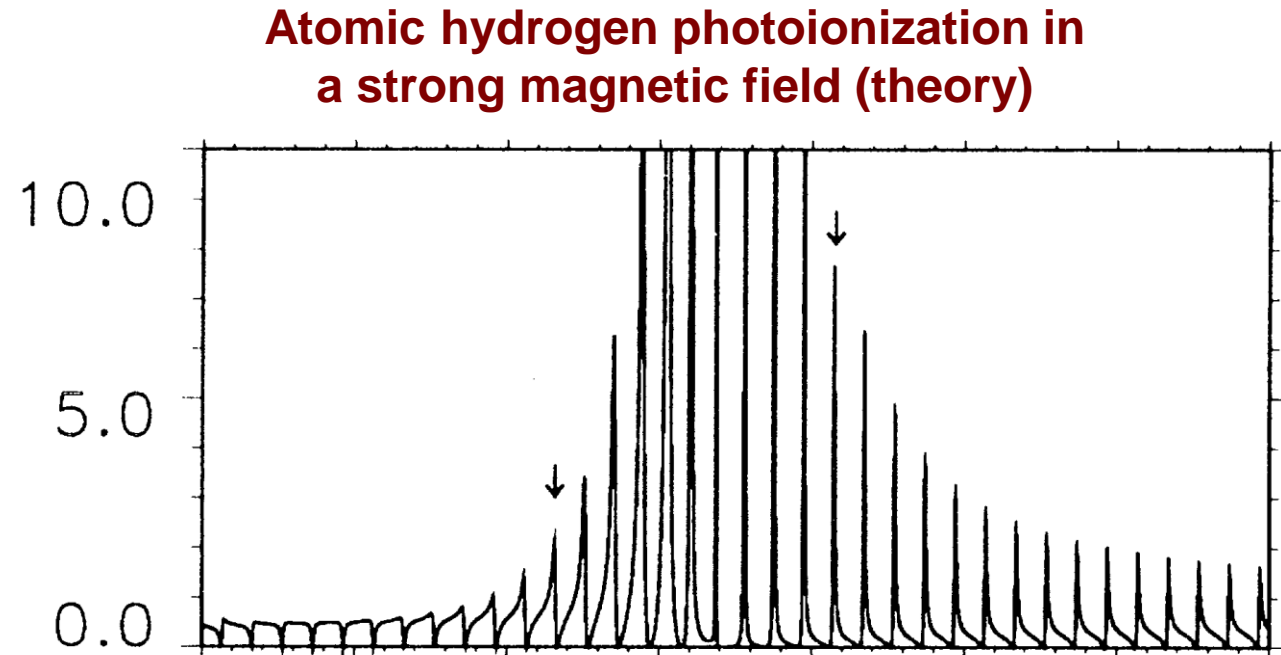
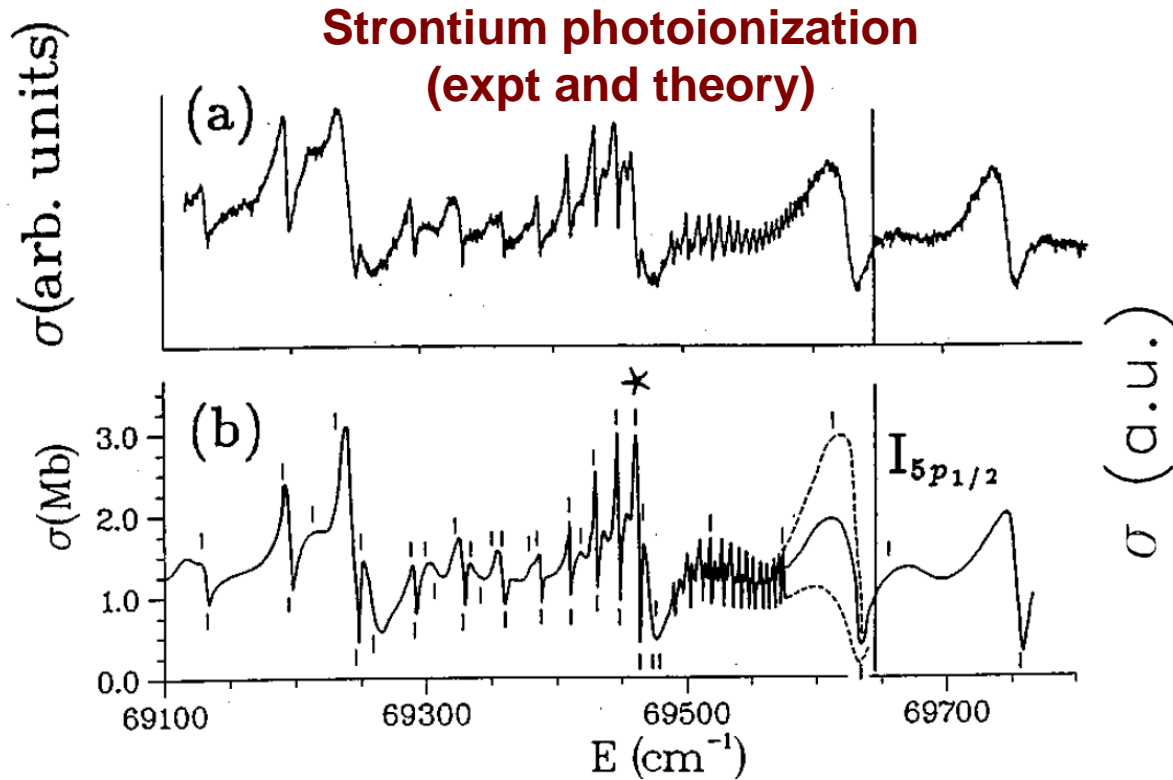
**Fig. 2. Mapping of Fano's  $q$  (line-shape asymmetry) parameter to the temporal response-function phase  $\varphi$ .** A bijective map between the two parameters is obtained in a range  $[-\pi, \pi]$ , while the function is periodic in  $2\pi$ . Lorentzian line shapes are obtained for the extreme cases of  $\varphi \rightarrow 2n\pi$  (integer  $n$ ), corresponding to  $q \rightarrow -\infty$  and  $q \rightarrow +\infty$ , respectively, whereas between these regimes Fano line shapes are obtained, with the special case of a window resonance at  $\varphi = (2n + 1)\pi$ ,  $q = 0$ . **(Insets)** The absorption line shapes  $\sigma(\varepsilon)$  (as depicted in Fig. 1)



for selected values of  $q(\varphi)$ . The laser interaction creates an additional phase shift (horizontal arrows) that changes the character of the observed resonance line shape. The dots represent the situations measured in the experiment and shown in Fig. 3. The shaded areas represent the errors which are given by the experimental uncertainty in the intensity determination.

While many systems show simple Fano resonances in the energy domain, as shown above, atomic spectra often show richer varieties of spectral shapes and patterns, which are virtually guaranteed to exist for multichannel Rydberg spectra.

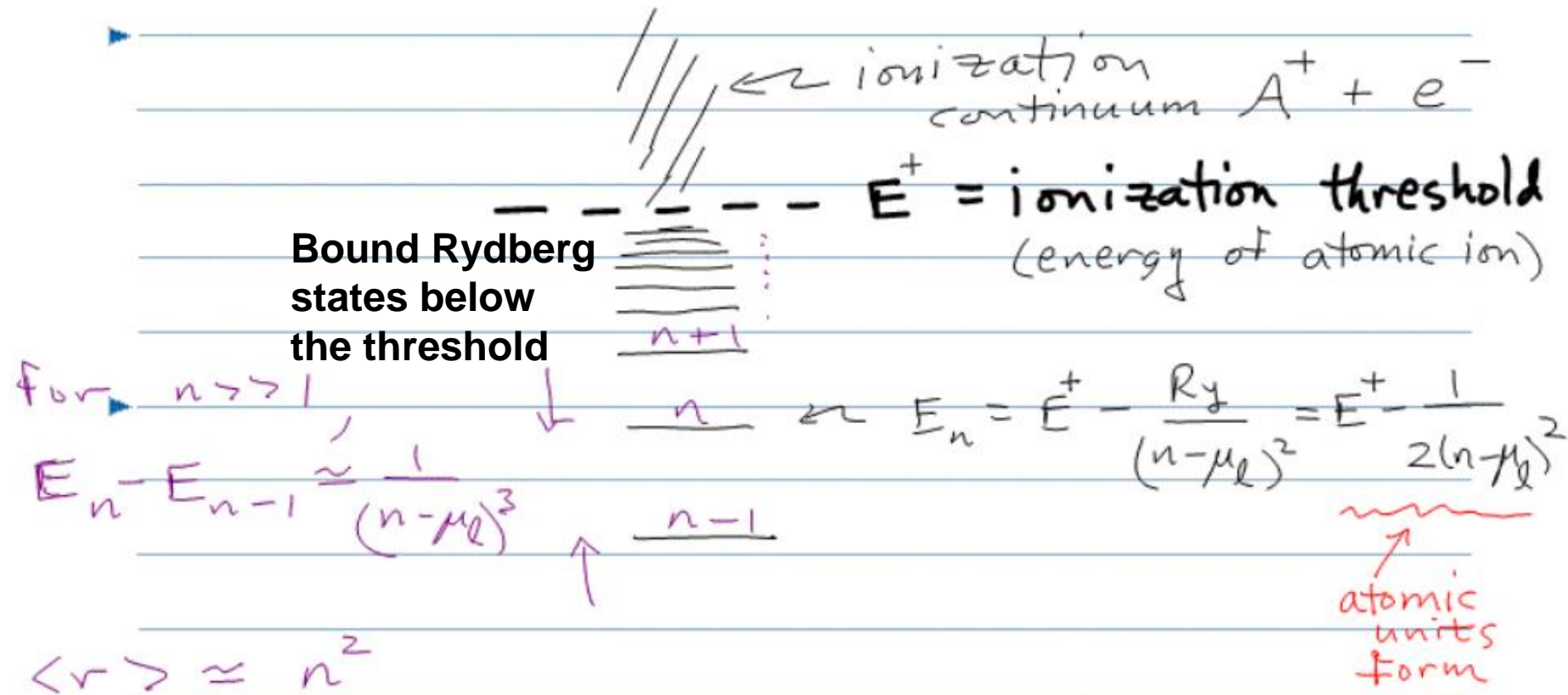
Here are some examples of such spectra observed and computed by realistic theory:



With rich spectra of this type, it becomes tedious and inefficient to characterize each individual resonance as a Fano lineshape. More desirable is to develop a theory that can describe the full spectrum across this entire energy range: multichannel quantum defect theory (MQDT)

# Multichannel Rydberg Systems

Before discussing the multichannel Rydberg problem, consider the main properties of a single-channel Rydberg series, as seen in photoabsorption:



# Precision measurements of quantum defects in the $nP_{3/2}$ Rydberg states of $^{85}\text{Rb}$

B Sanguinetti, H O Majeed, M L Jones and B T H Varcoe

J. Phys. B: At. Mol. Opt. Phys. 42 (2009) 165004

B Sanguinetti et al

**Table 2.** Measured frequencies for the  $nP_{3/2}$  states and respective quantum defects.  $E_n$  is measured from the centre of mass of the lower and upper states and contains a small correction to the wavemeter calibration. The third step data are reported exactly as measured.

$n$	Third step (MHz)	$E_n$ (MHz)	quantum defect $\delta = \mu$	$\delta$ Error ( $\times 10^{-5}$ )
36	236 496 706	1007 068 254	2.641 87	2.3
37	236 666 310	1007 237 858	2.641 79	2.5
38	236 821 728	1007 393 277	2.641 70	2.7
39	236 964 479	1007 536 027	2.641 75	2.9
40	237 095 926	1007 667 475	2.641 77	3.2
41	237 217 235	1007 788 783	2.641 73	3.4
42	237 329 406	1007 900 954	2.641 76	3.7
43	237 433 360	1008 004 909	2.641 62	4.0
44	237 529 853	1008 101 402	2.641 60	4.3
45	237 619 595	1008 191 144	2.641 56	4.6
46	237 703 191	1008 274 740	2.641 63	5.0
47	237 781 211	1008 352 760	2.641 51	5.3
48	237 854 117	1008 425 666	2.641 54	5.7
49	237 922 362	1008 493 911	2.641 48	6.1
50	237 986 322	1008 557 870	2.641 55	6.5
51	238 046 352	1008 617 901	2.641 67	6.9
52	238 102 791	1008 674 339	2.641 44	7.3
53	238 155 879	1008 727 427	2.641 61	7.8
54	238 205 906	1008 777 455	2.641 59	8.2
55	238 253 103	1008 824 651	2.641 39	8.7
56	238 297 662	1008 869 210	2.641 39	9.2
57	238 339 780	1008 911 329	2.641 48	9.8
58	238 379 637	1008 951 185	2.641 58	10.3
59	238 417 400	1008 988 949	2.641 41	10.9
60	238 453 197	1009 024 746	2.641 51	11.5

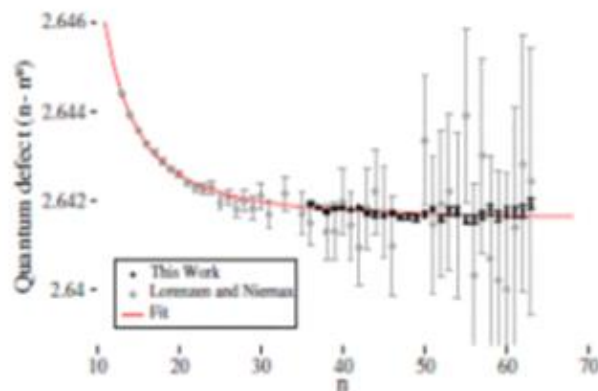


**Figure 6.** Quantum defects from the three different fitting methods. Data points for  $n = 5$  and  $n = 6$  were included in the calculations but are not shown, as their quantum defects are off the scale: 2.707 178 and 2.670 358, respectively.

meaning of the parameters. The following three different fitting procedures were implemented in the analysis of our data.

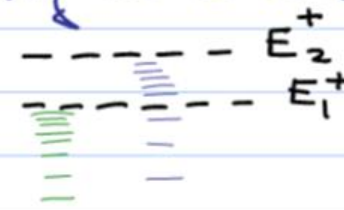
**Method 1.** The first method uses a simple fit routine. The quantum defect can be obtained as a function of  $n$  if we approximate  $\delta(n)$  by  $\delta_0$  [20]:

$$\delta(n) = \delta_0 + \frac{a}{(n - \delta_0)^2} + \frac{b}{(n - \delta_0)^4} + \dots \quad (6)$$

$\mu$  is nearly independent of  $n$

But in more complicated atoms having multiple ionization thresholds, the physics gets significantly more complicated, and richer.

simplest case of  $\rightarrow$  noninteracting Rydberg series



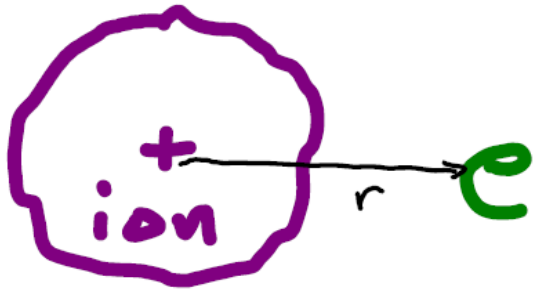
Note that for every energy level of an atomic ion, the neutral atom will possess an infinite Rydberg series of bound (or autoionizing) levels plus an adjoining ionization continuum



Beyond Simple Isolated Resonance Theory, to the idea of the:

COMPLEX RESONANCE (First consider 1-channel)

~ Consider an electron interacting with a positive ion with energy levels  $E_i$



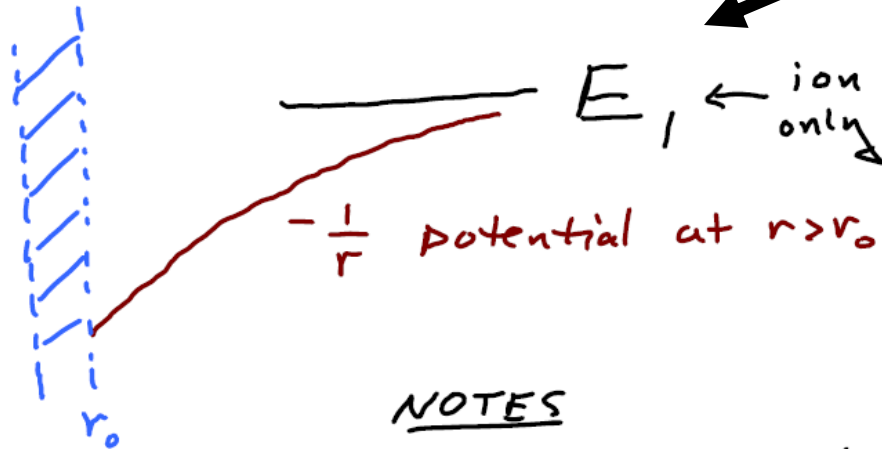
The Hamiltonian for this system can be written as

$$H = H_{ion} + h_e + V^{sr}(r)$$

with  $H_{ion} = |1\rangle E_1 \langle 1|$

$$h_e = T_e - \frac{1}{r}$$

$$V^{sr}(r) = \text{nonzero only at } r < r_0$$



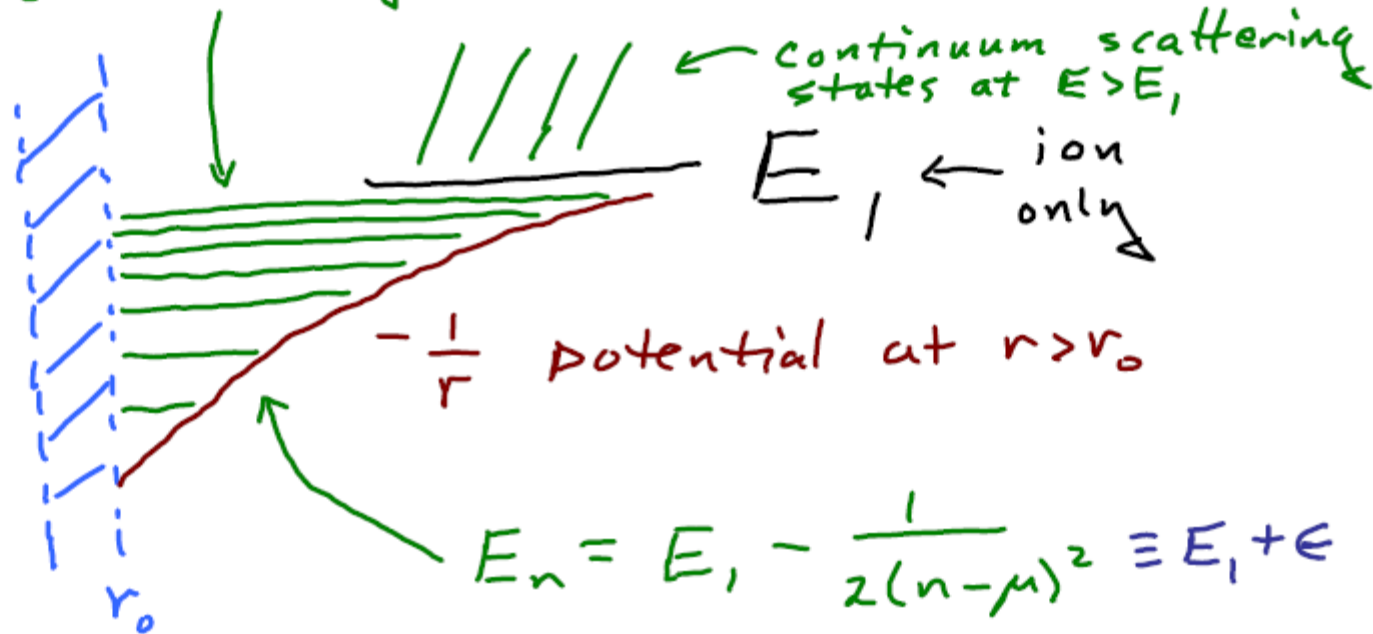
Think in terms of effective channel potentials

NOTES

- The long-range potential need not be Coulomb, as these effects occur also, e.g. in ultracold collisions
- This scenario here is referred to as "QUANTUM DEFECT THEORY"

$$V \longrightarrow -C_6/R^6 \text{ (van der Waals at long range for ultracold atom-atom collisions)}$$

single channel Rydberg levels at  $E < E_1$



$-\frac{1}{r}$  potential at  $r > r_0$

$$E_n = E_1 - \frac{1}{2(n-\mu)^2} \equiv E_1 + \epsilon$$

$\mu =$  quantum defect, would vanish if  $v^{sr} \rightarrow 0$

Unnormalized solution ( $r > r_0$ )

If  $v^{sr} = 0 \rightarrow f_\epsilon(r)$

If  $v^{sr} \neq 0 \rightarrow f_\epsilon(r) - g_\epsilon(r) \tan \delta$

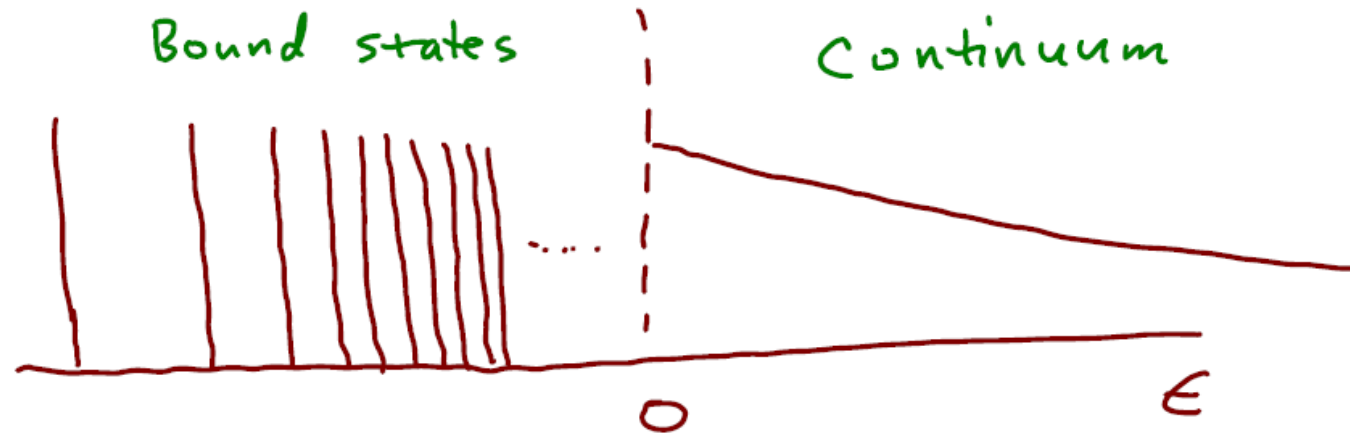
$\mu =$  energy-independent

Note: call  $\nu = (-2E)^{-1/2} =$  effective quantum number

Seaton, others:  $\delta \equiv \pi \mu$

scattering phaseshift gives bound quantum defects!

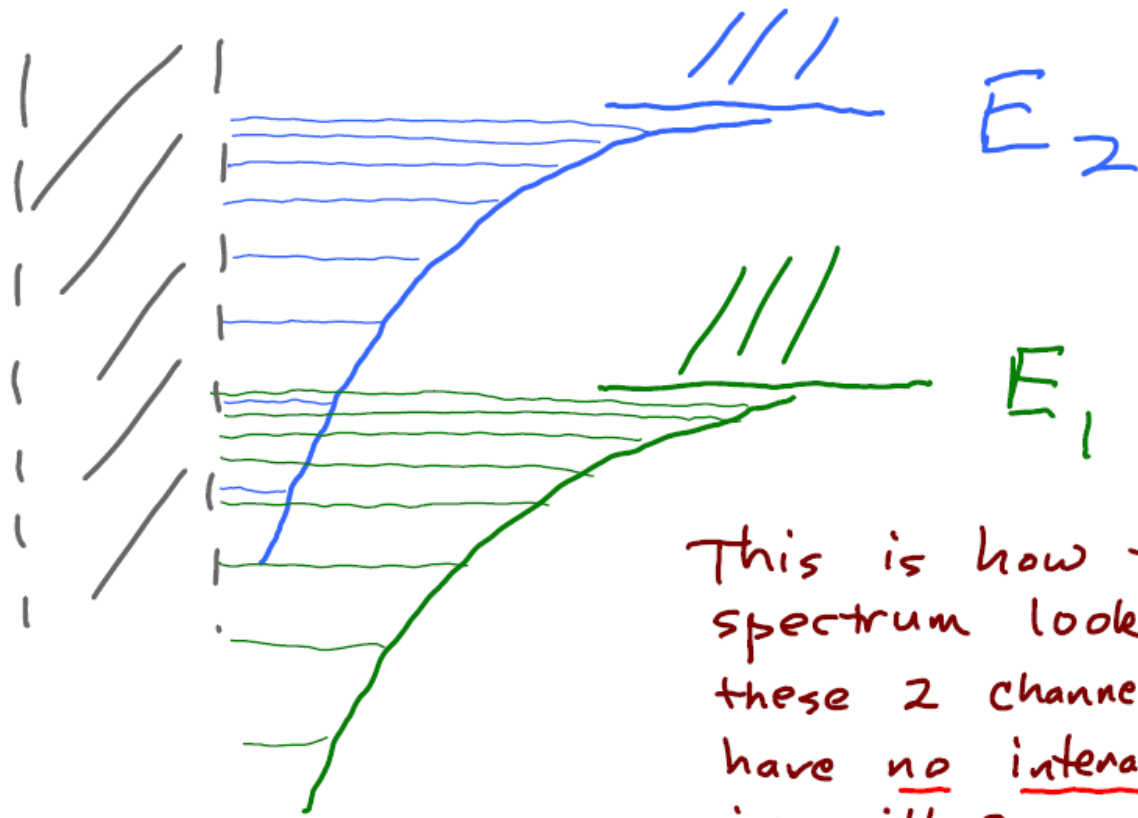
Single channel photoabsorption oscillator strengths



## Multichannel generalization

Of course an atomic or molecular ion often has 2 or more energy eigenstates  $E_i$  in the range of interest, e.g. with 2 channels this looks like





This is how the atom spectrum looks if these 2 channels have no interaction, i.e. with 2 separate regular Rydberg series "unperturbed"

$\Rightarrow$  If no interaction, each eigenstate belongs to either channel 1 or channel 2

IN practice there will always be some interaction unless the channels have different symmetries



## Effects of interactions between 2 channels

- bound state energy level perturbations at  $E < E_1$
- autoionization of levels in region  $E_1 < E < E_2$
- elastic and inelastic collisions at  $E > E_2$

we're used to this situation in ordinary collision theory  $\Rightarrow$  we need a scattering matrix  $\begin{pmatrix} S_{11} & S_{12} \\ S_{21} & S_{22} \end{pmatrix}$

The  $i'$ -th independent solution at energy  $E$  at  $r > r_0$  is:

$$\Psi_{i'}^s = A \sum_i |i\rangle \left( \underbrace{f_i^-(r)}_{\substack{\uparrow \\ \text{incoming} \\ \text{radial wave}}} S_{ii'} - \underbrace{f_i^+(r)}_{\substack{\uparrow \\ \text{outgoing} \\ \text{radial wave}}} S_{i'i'} \right)$$

or we often like to work with real representations of scattering amplitudes and information, i.e. the K-matrix, related to S by

$$\underline{S} = \frac{\underline{1} + i\underline{K}}{\underline{1} - i\underline{K}}, \quad \underline{K} = \text{real, symmetric}$$

$$\underline{\Psi}_{i'}^k = A \sum_i |i\rangle (f_i(r) \delta_{ii'} - g_i(r) K_{ii'})$$

where  $K_{ii'}(E)$  depends only weakly on  $E$  and for our analysis can be assumed constant

The most interesting spectral region for a 2-channel problem is the autoionization region  $E_1 < E < E_2$

Remarkably, the same constant K matrix at  $E > E_2$  applies at  $E < E_2$ , but we need one extra step, the famous MQDT closed channel elimination:

Why "eliminate" channel 2? ←

- Because at  $E < E_2$ ,  $(f_2, g_2)$  both grow exponentially, i.e.

$$f_i(r) \rightarrow \sin \pi \nu_i e^{k_i r} (\dots) + e^{-k_i r} (\dots)$$

$$g_i(r) \rightarrow -\cos \pi \nu_i e^{k_i r} (\dots) - e^{-k_i r} (\dots)$$

and we must form a linear combination of  $\Psi_1^k$  and  $\Psi_2^k$  that kills the exponential growth,

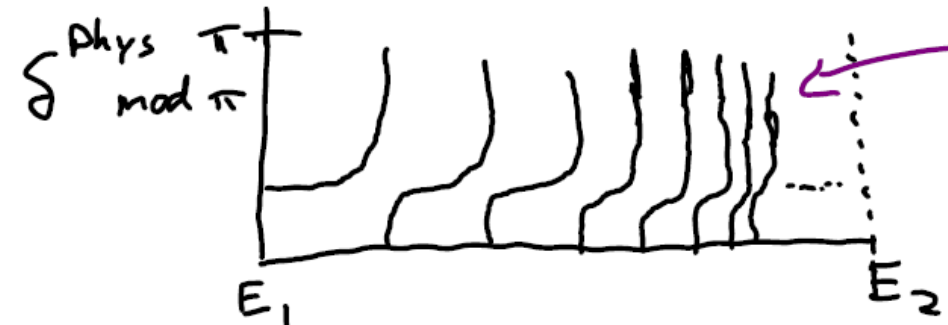
This is loose language, because Channel 2 has not truly been eliminated from the problem, only its exponential growth at infinity has been "eliminated"!

There will remain physically important wave functions in Channel 2, but after the "elimination step" those wave functions will decay exponentially as they must!

giving the physical phaseshift at  $E_1 < E < E_2$  as:

$$\tan \delta^{phys}(E) = K_{11} - K_{12} (K_{22} + \tan \pi \nu_2)^{-1} K_{21}$$

Some mathematics has been skipped that produces this equation, but it is relatively simple. See, e.g. Seaton, Rep. Prog. Phys. 46, 167 (1983)



each rise by  $\pi$  signals a new autoionizing resonance

or in photoabsorption, we see a simple Rydberg series of autoionizing Fano resonances

U. Fano, Phys. Rev. 124, 1866 (1961)



**Note that MQDT describes this infinity of Rydberg autoionizing levels near threshold  $E_2$  with just 3 real elements of the symmetric  $2 \times 2$  K-matrix plus two (nearly constant) electric dipole matrix elements.**

each Fano lineshape looks like  $\sigma_n = \sigma_{BG} \frac{\left( q + \frac{E - E_n}{\frac{1}{2}\Gamma_n} \right)^2}{1 + \left( \frac{E - E_n}{\frac{1}{2}\Gamma_n} \right)^2}$

and  $\Gamma_n = \frac{\vec{F}^2}{V_n^3}$

Other observations

- If only one continuum, then each Fano resonance has a point where  $\sigma = 0$
- The phaseshift rises by  $\pi$  across each Fano resonance
- TIME DOMAIN IMPLICATIONS: see Ott et al. Science 340 716 (2013)

Now, the preceding discussion involved  
 "simple" resonances. Now we discuss  
 the **COMPLEX RESONANCE**,  
 and we need to consider at least  
 3 channels

Most of the mathematical details are worked out in the following article by Q. Wang & CHG, Phys. Rev. A 44, 1874 (1991). For earlier relevant work, see Giusti-Suzor and Fano, JPB 17, 215 (1984) and Friedrich & Wintgen, PRA 32, 3231 (1985)

We are mainly interested in the energy range  $E_1 < E < E_2$  between thresholds 1 and 2

$$v_i = [-2(E - E_i)]^{-1/2}$$

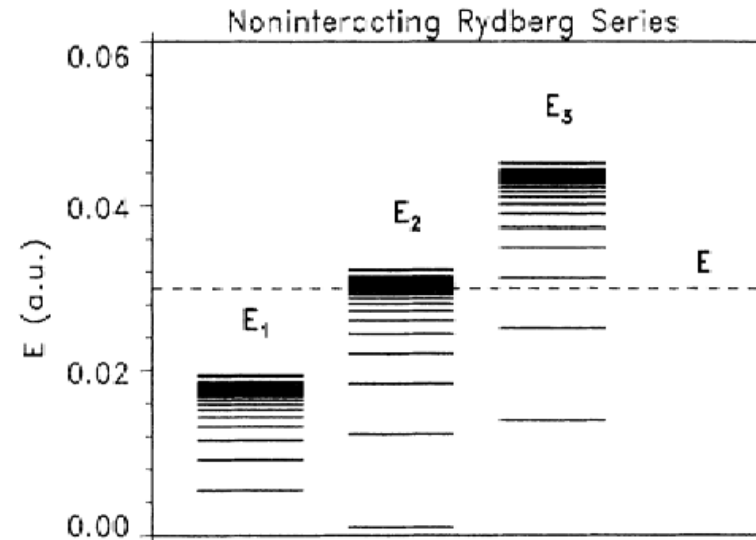


FIG. 1. Zeroth-order picture of a Rydberg series converging to three ionization thresholds  $E_1 < E_2 < E_3$ .

In fact we can first "eliminate" channel 3 to obtain energy-dependent 2-channel parameters, and then use our 2-channel math

$$\tilde{K} = \begin{bmatrix} K_{11} - \frac{K_{13}K_{31}}{T_3} & K_{12} - \frac{K_{13}K_{32}}{T_3} \\ K_{21} - \frac{K_{23}K_{31}}{T_3} & K_{22} - \frac{K_{23}K_{32}}{T_3} \end{bmatrix}$$

where  $T_i \equiv \tan \pi \nu_i + K_{ii}$

And for photoabsorption processes that probe these states, we need to introduce three constant dipole amplitudes  $d_1, d_2, d_3$ , and the channel elimination gives two energy dependent dipole amplitudes with a

$$\tilde{d} = \begin{bmatrix} d_1 - \frac{K_{13}d_3}{T_3} \\ d_2 - \frac{K_{23}d_3}{T_3} \end{bmatrix}$$

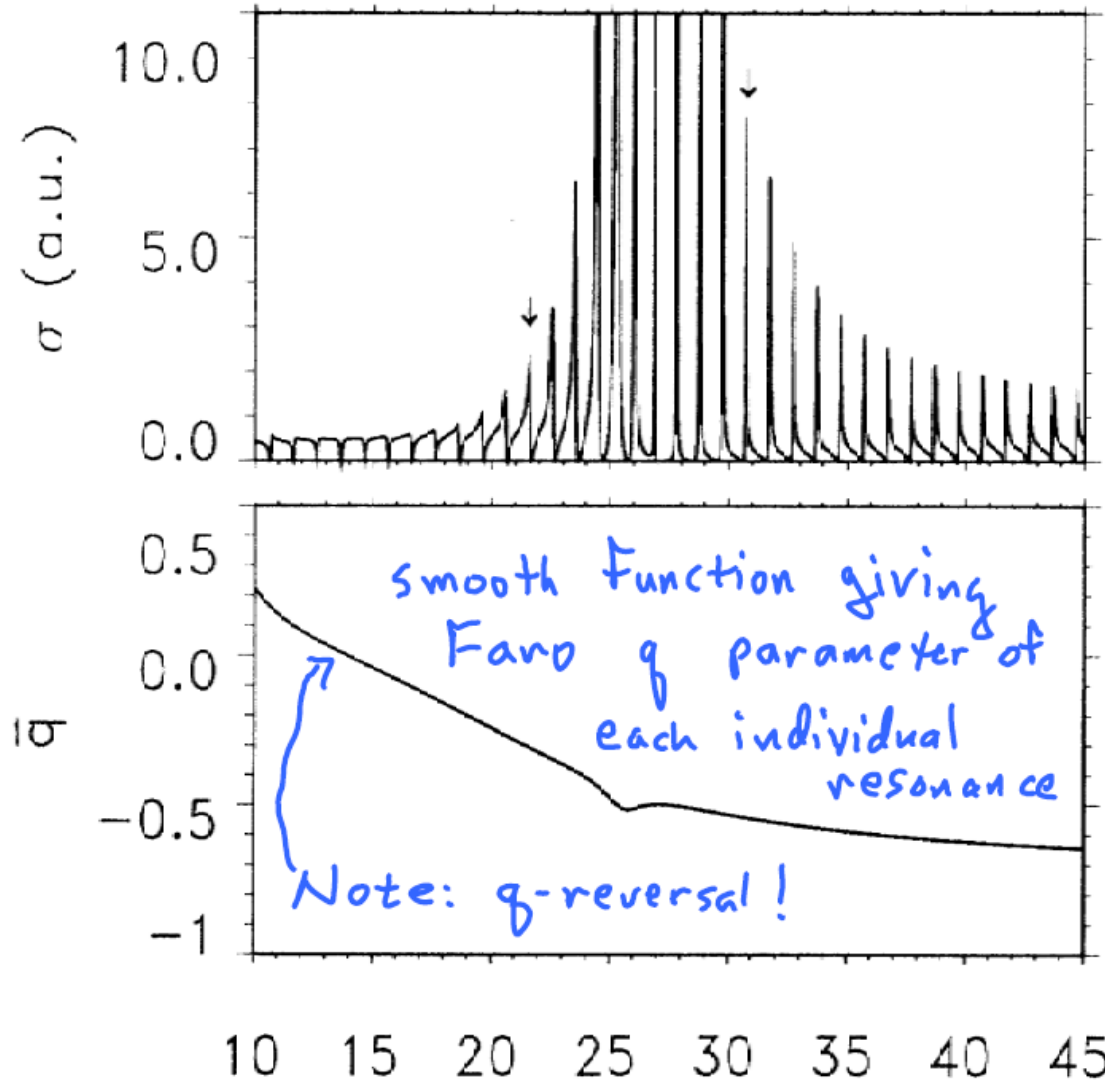
The energy-dependent photoabsorption cross section is given by

$$\sigma = I_0 \cos^2 \Delta \left[ \tilde{d}_1 - \frac{\tilde{K}_{12} \tilde{d}_2}{\tan \pi \nu_2 + \tilde{K}_{22}} \right]^2 \quad \text{where} \quad \tan \Delta = \tilde{K}_{11} - \frac{\tilde{K}_{12}^2}{\tan \pi \nu_2 + \tilde{K}_{22}}$$

So the cross section and physical phaseshift formulas are the same as for 2-channel QDT, except that now the  $\tilde{K}, \tilde{d}$  are themselves energy-dependent in a resonant way.



Here is an example spectrum across a single "complex resonance"



### Effects to note

- 1) The individual resonance widths vary across the complex resonance
- 2) One resonance has nearly zero width
- 3) The individual  $q$ -parameters change sign, called a " $q$ -reversal" effect

Interpretation of multiple time scales...

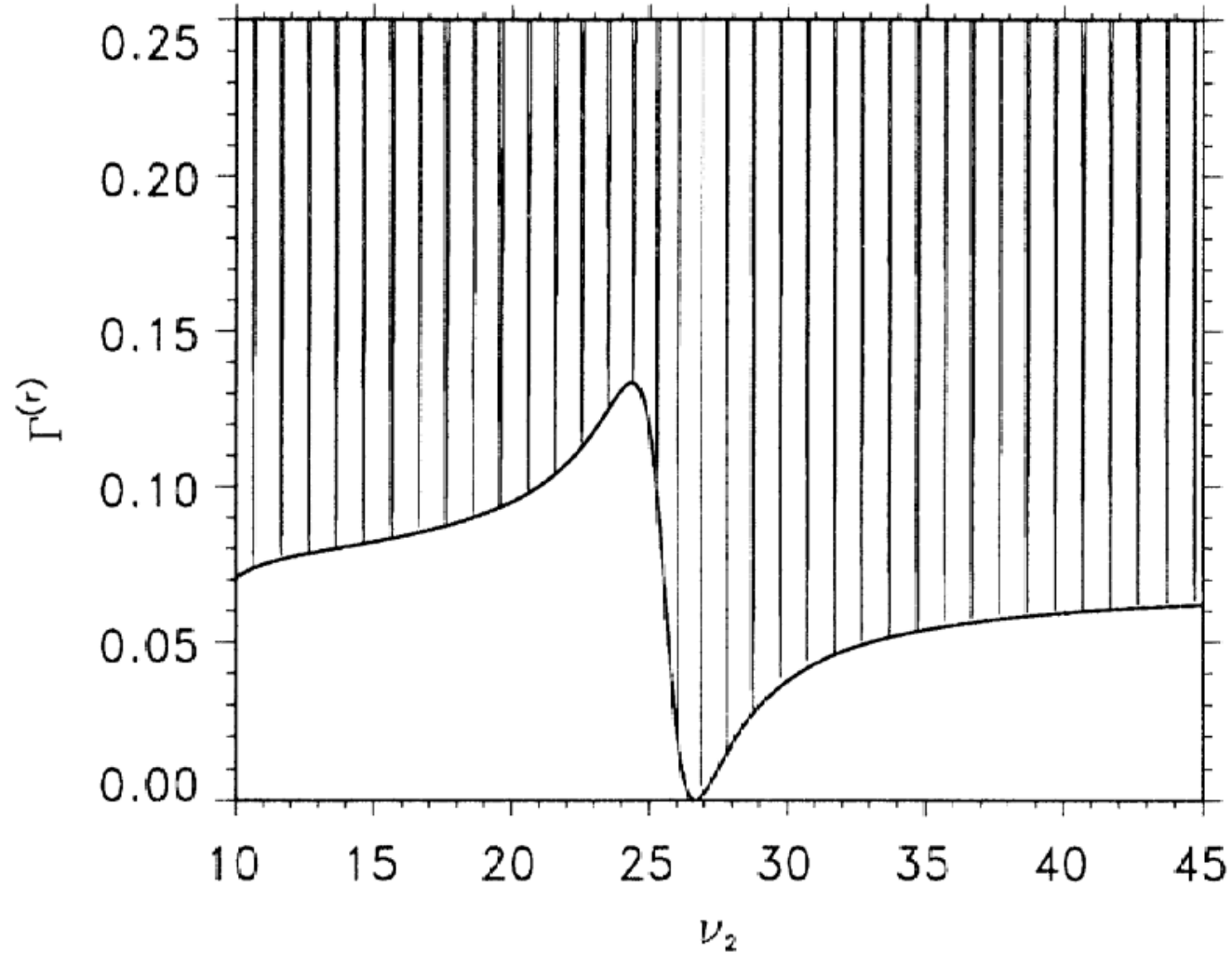
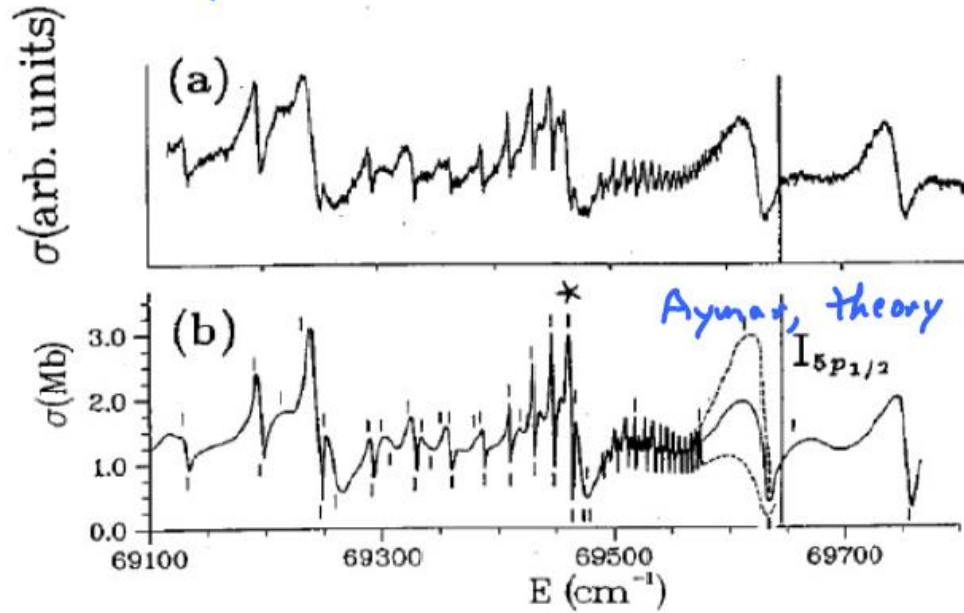


FIG. 5. The rapidly oscillating function is the reduced width function calculated from Eq. (9a). The solid curve is the smooth reduced width function.



Sr photoionization example Brown + Ginter, expt



H<sub>2</sub> photoionization Another complex Fano-Feshbach resonance studied by Jungen & Raouf, 1981

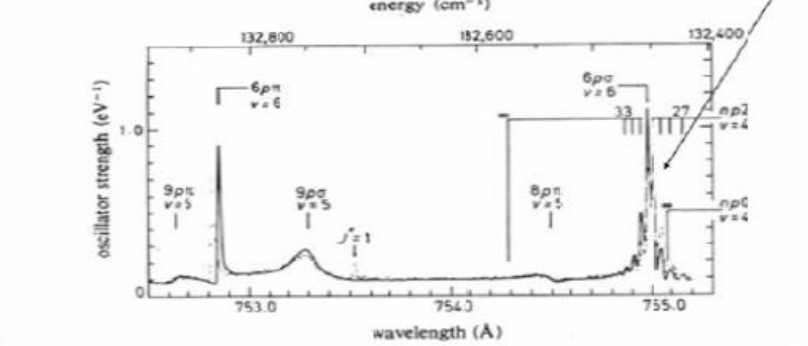
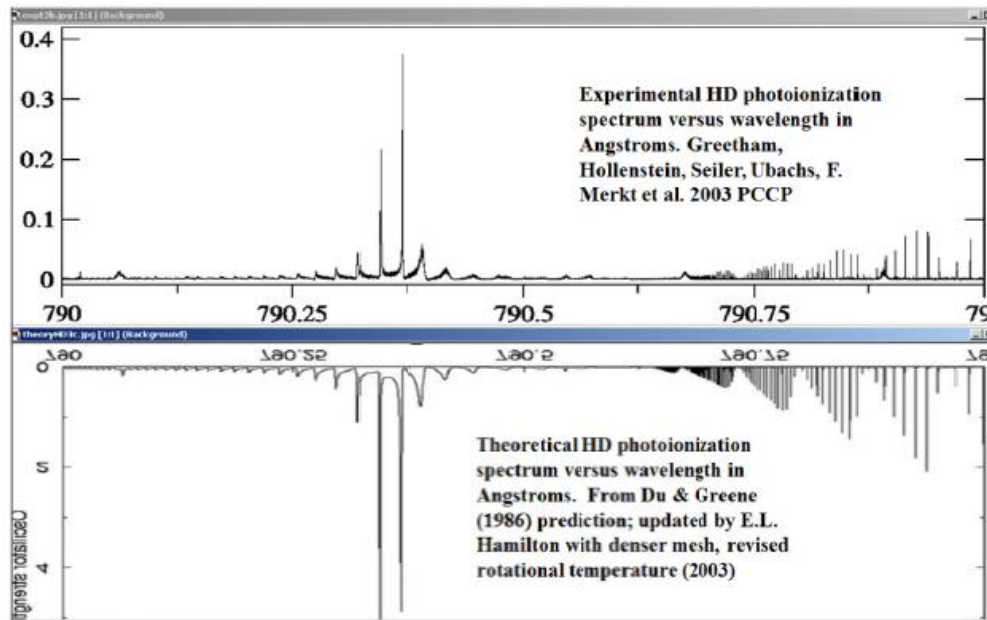


FIG. 10. Preionization near the  $v^+ = 4$ ,  $N^+ = 0$  and 2 thresholds in H<sub>2</sub> ( $J = 1$ ,  $J'' = 0$ ). The observed and calculated total oscillator strengths are shown as functions of photon wavelength. The experimental points from Dehmer and Chupka (1976) have been shifted by  $-0.06\text{\AA}$  so as to bring the observed and calculated 9p $\sigma$ ,  $v = 5$  peaks into coincidence. The calculated spectrum is broadened to a resolution of  $0.015\text{\AA}$  to correspond to the experimental measurements. (After Jungen and Raouf, 1981.)

HD photoionization example



Good examples of complex multichannel Rydberg resonances observed in various systems

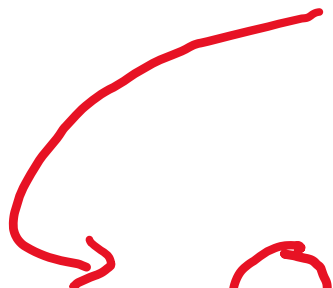
Most of the mathematical details are worked out in the following article by Q. Wang & CHG, Phys. Rev. A 44, 1874 (1991). For earlier relevant work, see Giusti-Suzor and Fano, JPB 17, 215 (1984) and Friedrich & Wintgen, PRA 32, 3231 (1985)

# A further insight into the physics contained in multichannel Rydberg physics

- Use of the Wigner-Smith time-delay matrix to analyze resonance properties
- Recall that the scattering matrix in a single-channel system can be characterized by a phaseshift  $\delta$  as

$$S = \exp(2i\delta)$$

Eugene Wigner showed that a time-dependent wavepacket that is scattered from a spherically symmetric potential experiences a time delay compared to a non-interacting system that is equal to


$$Q = 2\hbar \frac{d\delta}{dE}$$

Wigner, E. P., 1955, Phys. Rev. 98, 145

$$Q = i\hbar S \frac{d}{dE} S^\dagger$$

Multichannel generalization by  
F. T. Smith, 1960, Phys. Rev. 118, 349

Recall that at a resonance in some symmetry for any system, the sum of the eigenphases increases by  $\pi$  as the energy increases through the resonance. The energy derivative of the eigenphase sum looks Lorentzian for an isolated resonance. This can be expressed in terms of the time delay matrix as the  $\text{trace}(\underline{Q})$ , as can be seen in some examples from atomic physics taken from our 1996 Rev. Mod. Phys. Article (Aymar et al.), e.g. in barium doubly excited states studied in photoionization:

Two resonances studied on the real energy axis through analysis of the time delay matrix in Ba. This symmetry has an 18 x 18 S-matrix computed using MQDT and R-matrix theory, but each resonance is dominated by just one of the eigenphases.

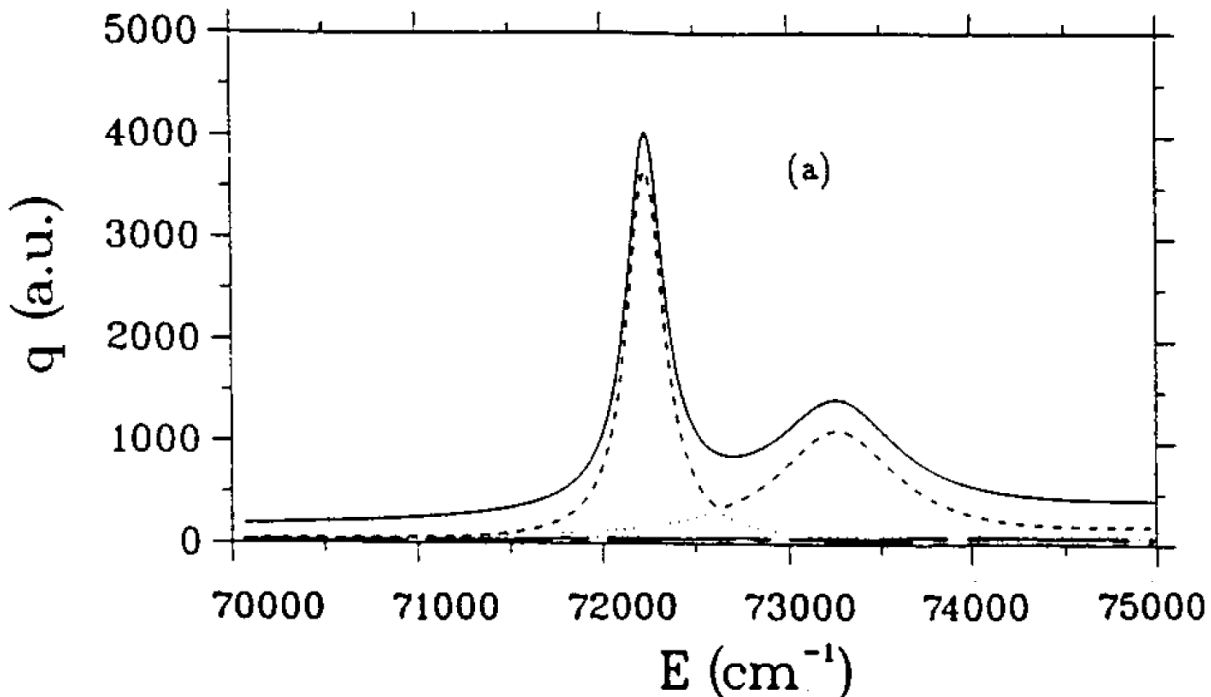
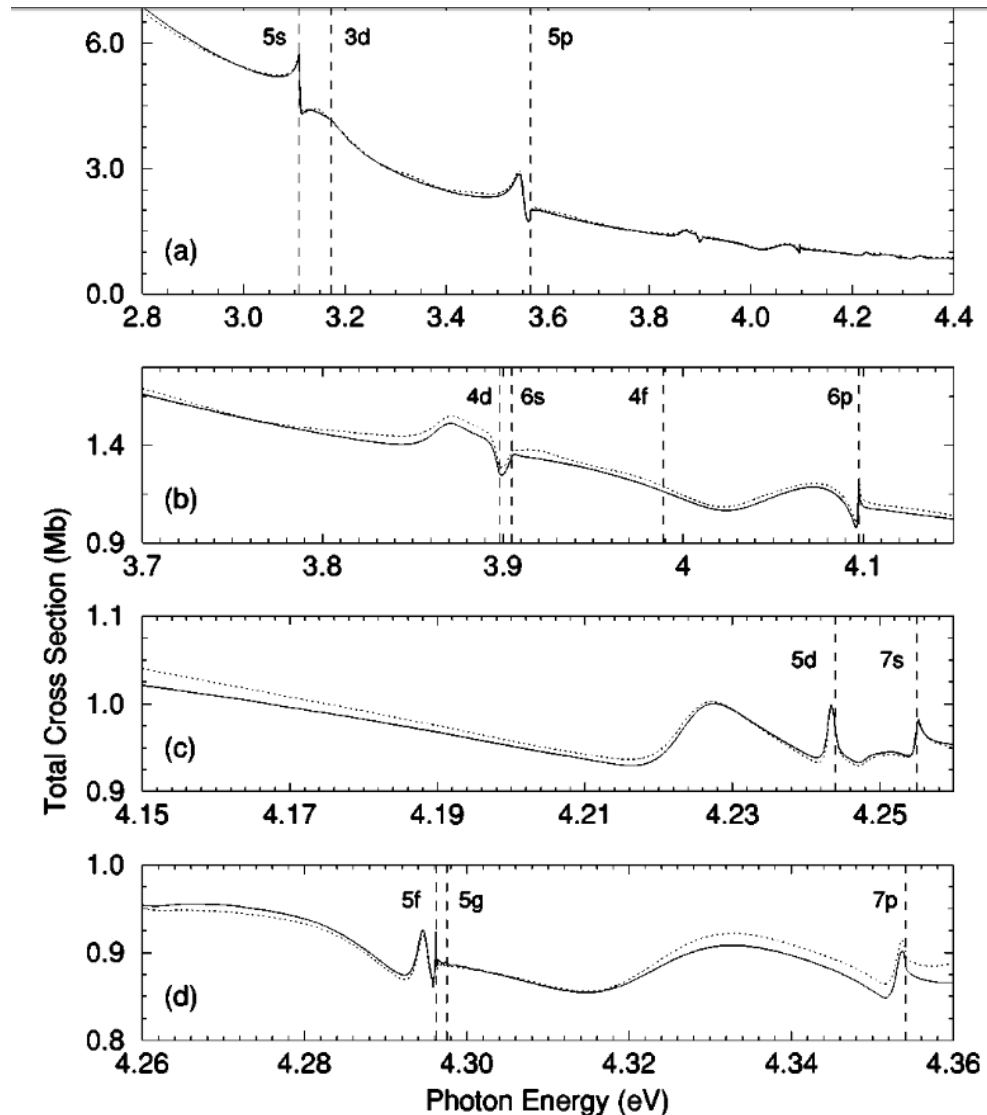


FIG. 20. The Ba  $6d^2 \ ^3F_4$  and  $^1G_4$  resonances: (a) sum of eigenvalues  $q$  of the time-delay matrix  $\underline{Q}$  identical to  $\text{Tr}\underline{Q}$  (full line) and individual eigenvalues  $q$  (18 other lines)—note that the curves associated with 16 eigenvalues are almost superim-

The eigenvector of  $\underline{Q}$  corresponding to the dominant eigenphase of each resonance (at the energy where it is maximum) provides us with the probabilities of decay into the different individual decay channels. This is sometimes expressed as the partial width of the resonance in each open channel, obtained by multiplying the squared eigenvector components by the total width of the resonance

Note also that  $\underline{Q}$  can be viewed as a density of states matrix, see our RMP 1996

These ideas are valid more generally than for the context of Rydberg states, that are characterized by a long range attractive Coulomb potential between the electron and the residual atomic or molecular ion. Here is an example that we have studied in negative ion photodetachment that shows many resonances in the  $K^-$  ion:

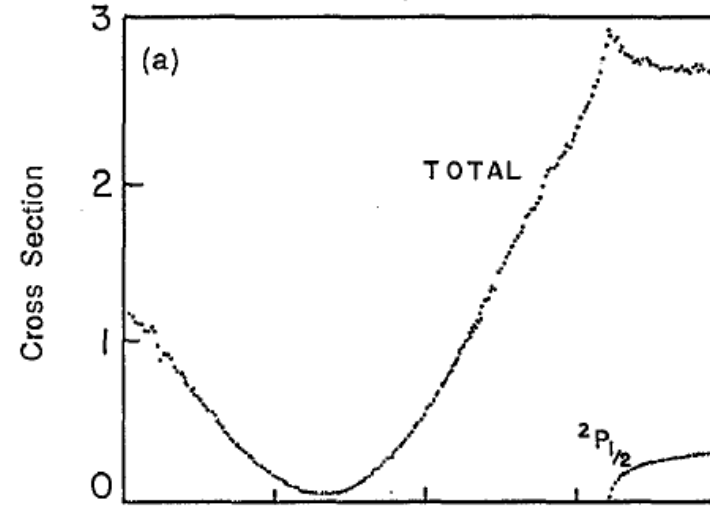
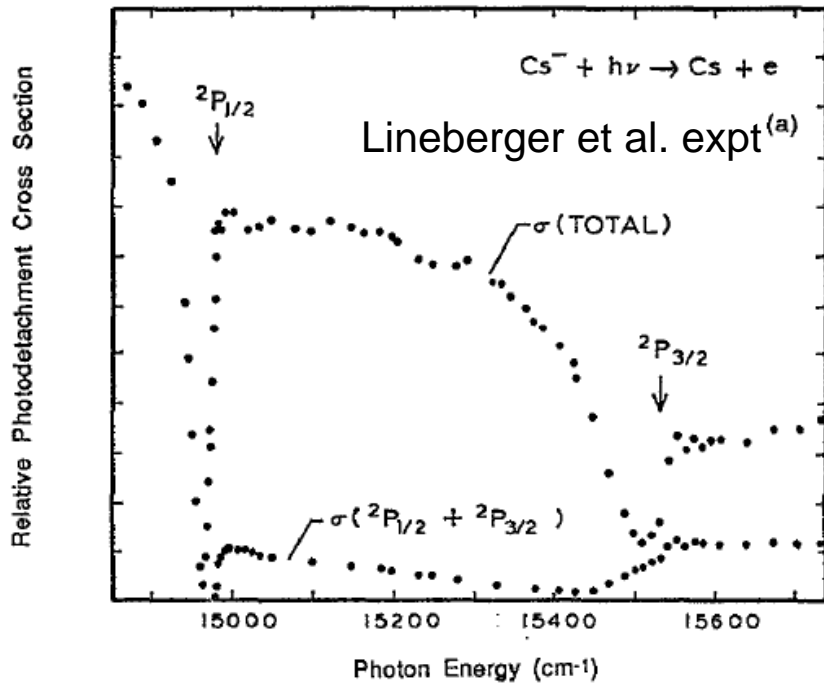


Total  $K^-$  photodetachment cross sections (length and velocity) computed by Liu (PRA 2001) using R-matrix and long range multichannel coupling methods.

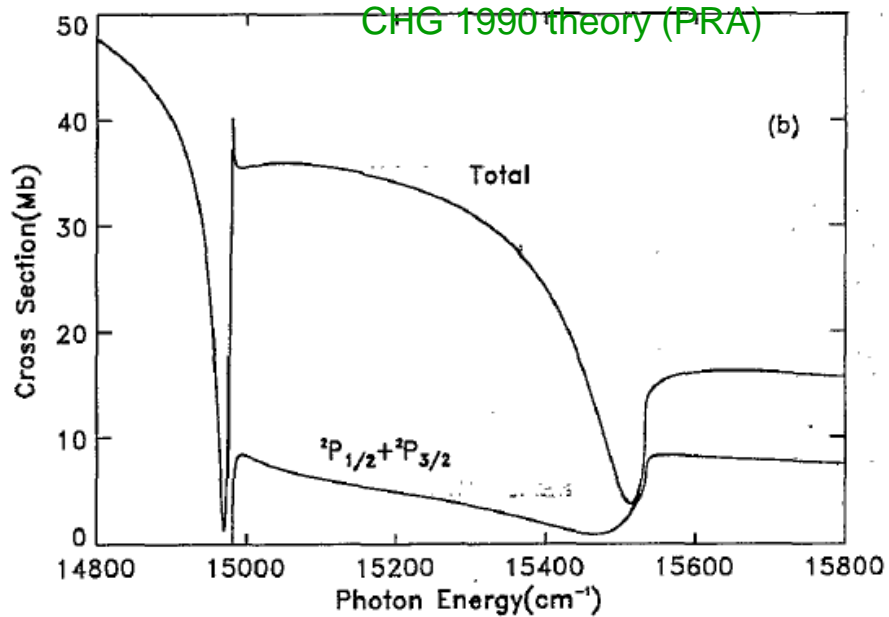
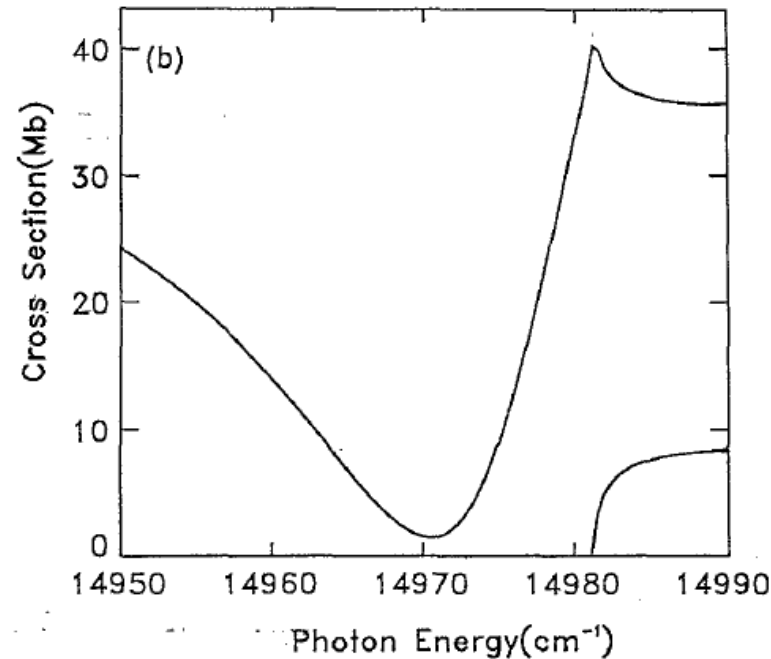
In this study, Liu noted the interesting huge negative polarizability of  $K(5g)$ , and this may have stimulated the Hanstorp group to explore the implications of this unusual long-range repulsion on the near-threshold behavior in their 2012 PRL.

Eiles & CHG (2019 PRL) carried out a detailed analysis of new experiments to extract dominant decay channels and the resonance classification.

**Photodetachment of the Cs<sup>-</sup> negative ion, showing how a Fano resonance overlapping a threshold region has its lineshape distorted**



**Note the Wigner threshold law cusp observed at the 6p(1/2) detachment threshold**





# Ultracold Atomic Physics

(1) Controlled 2-body interactions

- Fano-Feshbach resonances in Rb-Rb (in 3D)
- Confinement-induced resonances (effectively 1D)

(2) Universal Efimov physics (3 identical bosons in 3D)

- zero range theory

Efimov Physics: a review by P Naidon, S Endo  
Reports on Progress in Physics 80 (5), 056001 2017

- van der Waals universality

(3) N-body clusters and recombination

- 4 body universal resonances
- 5 body resonances

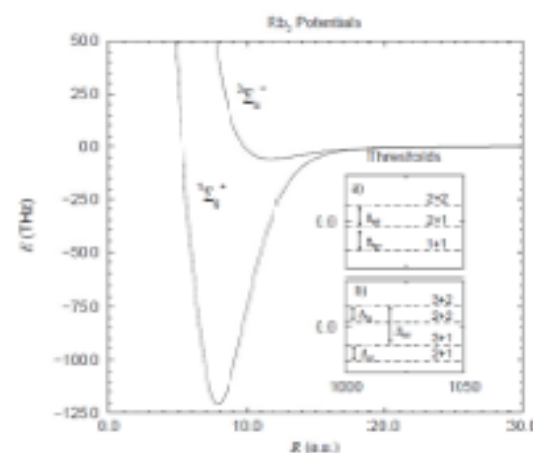
(4) Beyond ultracold atoms

- the 3-nucleon problem

# (1) Controlled 2-body interactions

- Fano-Feshbach resonances in Rb-Rb (in 3D)

Consider the Hamiltonian for 2 Rb atoms:



Quantum chemistry normally ignores hyperfine structure and calculates the singlet ( $S=0$ ) and triplet ( $S=1$ ) potential curves in the Born-Oppenheimer approximation.

$$\text{i.e. } V_{\text{elec}}(R) = \sum_{S=0}^1 \sum_{M_S} |SM_S\rangle V^{(S)}(R) \langle SM_S|$$

*SM<sub>S</sub> = good quantum numbers*

$$\text{e.g. } |SM_S\rangle \equiv \sum_{m_1, m_2} |s_1 m_{s_1}\rangle |s_2 m_{s_2}\rangle \langle s_1 m_{s_1}, s_2 m_{s_2} | SM_S\rangle$$

But Rb has hyperfine interaction between the nuclear spin ( $i, m_i$ ) and the electron spin ( $s, m_s$ ),

$$\Rightarrow H^{\text{hf}} = \mathcal{C}_1 (\vec{i}_1 \cdot \vec{s}_1) + \mathcal{C}_2 (\vec{i}_2 \cdot \vec{s}_2)$$

*Good quantum numbers are  $f_1, f_2$*

or

$$H^{\text{hf}} = \Lambda_a \frac{\Delta_a}{2i_a + 1} (f_a^2 - i_a^2 - s_a^2) + \Lambda_b \frac{\Delta_b}{2i_b + 1} (f_b^2 - i_b^2 - s_b^2) \quad \text{where } \Lambda_a + \Lambda_b = +1 \quad \text{and}$$

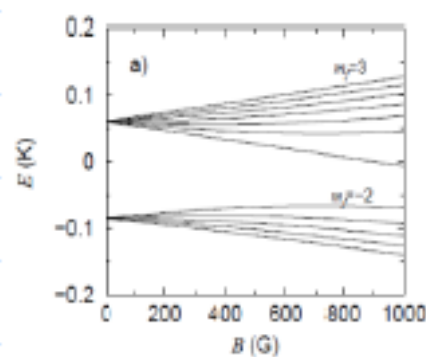
$$\Delta \approx 6.8 \text{ GHz } (^{87}\text{Rb}) \quad \text{or} \quad \Delta \approx 3.0 \text{ GHz } (^{85}\text{Rb})$$



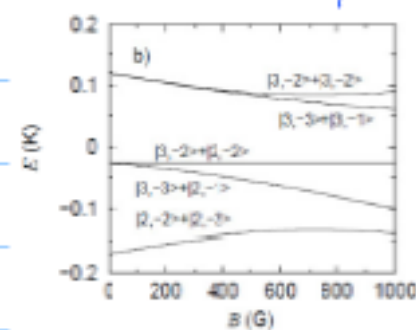
And since these systems are frequently studied in a magnetic field  $\vec{B} = B \hat{z}$ , we must also add the Zeeman  $H^B$ :

$$H^B = -B [g\mu_e(s_z^a + s_z^b) + \mu_N(g_N^a i_z^a + g_N^b i_z^b)]$$

← good quantum numbers are  $m_{S_1}, m_{S_2}, m_{I_1}, m_{I_2}$



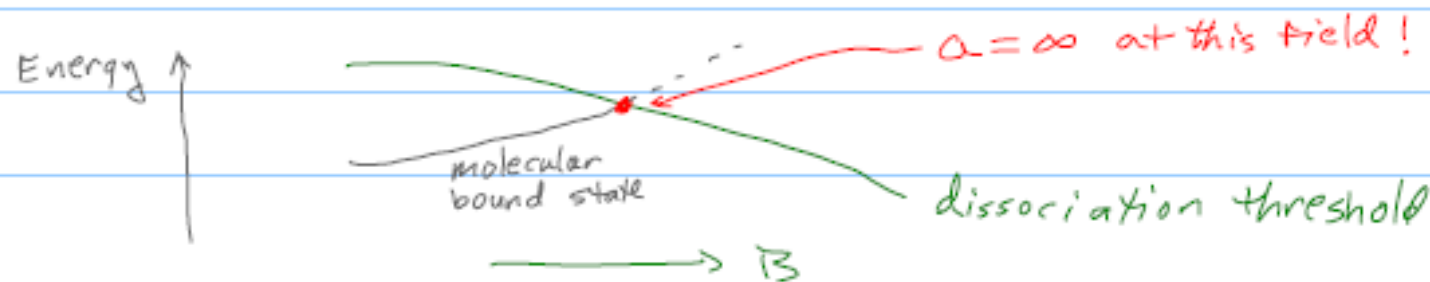
← These  $^{85}\text{Rb}$  atomic energies... combine for 2 atoms to give dissociation thresholds for  $^{85}\text{Rb}_2$

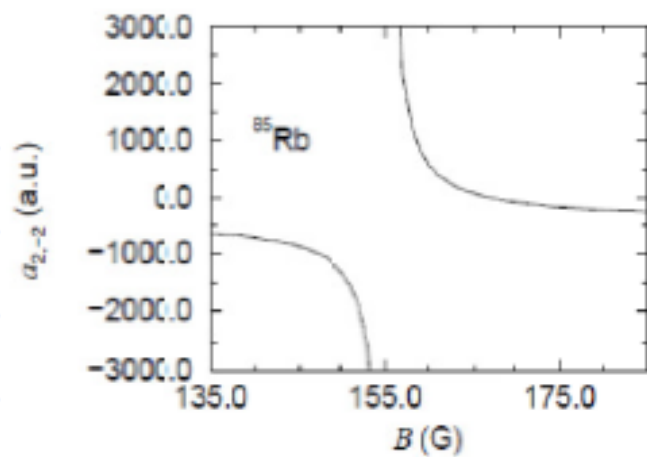


The key point: As one changes B-field some bound levels become unbound  $\Rightarrow$  resonances

And...

The scattering length diverges where a bound state has zero binding energy





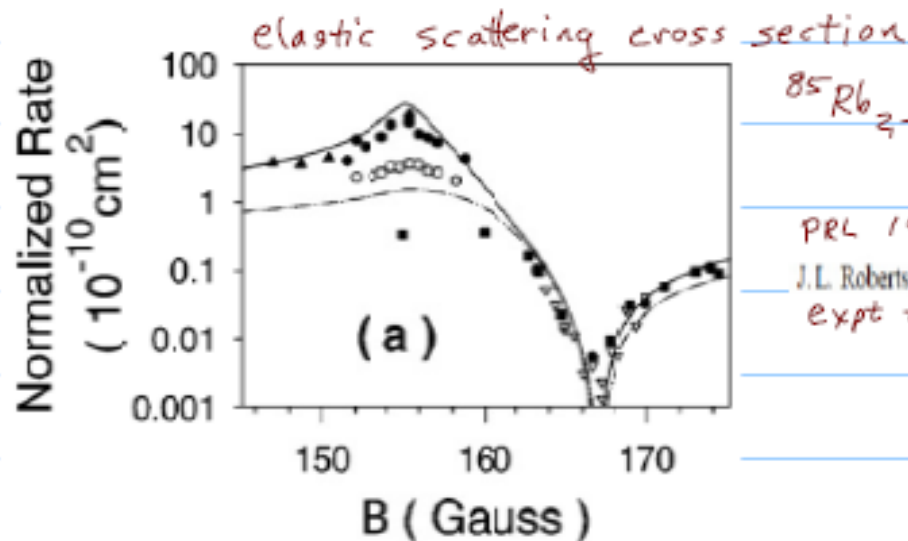
$\sim {}^{85}\text{Rb} - {}^{85}\text{Rb}$  Fano-Feshbach resonance

i.e. scattering length vs.  $B$ .

This is the most common way of modifying the atom-atom scattering length, with dramatic implications for the few-body and many-body BEC physics!

Alternative methods:

- laser- or rf-dressing of the atomic/molecular Ham.
- confinement-induced resonances



$${}^{85}\text{Rb}_{2,-2} + {}^{85}\text{Rb}_{2,-2} \quad \sigma = 8\pi a^2(B) \quad (\text{thermally averaged})$$

PRL 1998

J.L. Roberts, N.R. Claussen, James P. Burke, Jr., Chris H. Greene, E.A. Cornell,\* and C.E. Wieman  
expt + theory

**Berninger et al., highly detailed map of bound states and Fano-Feshbach resonances in Cs-Cs**

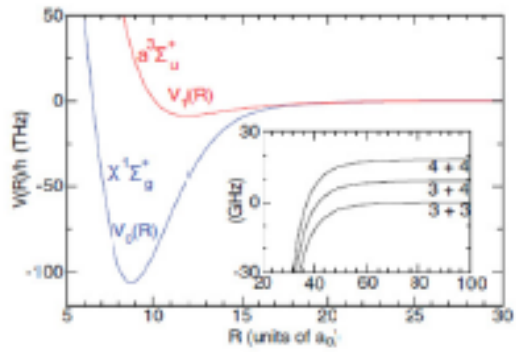
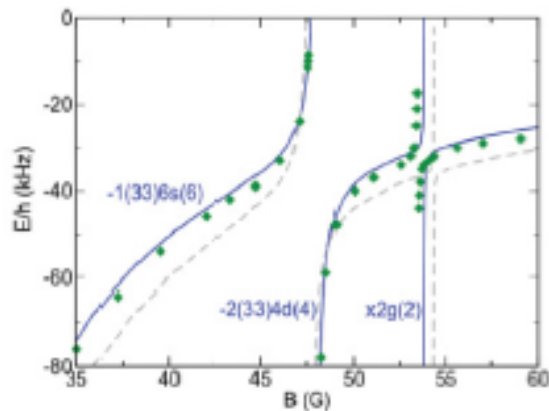
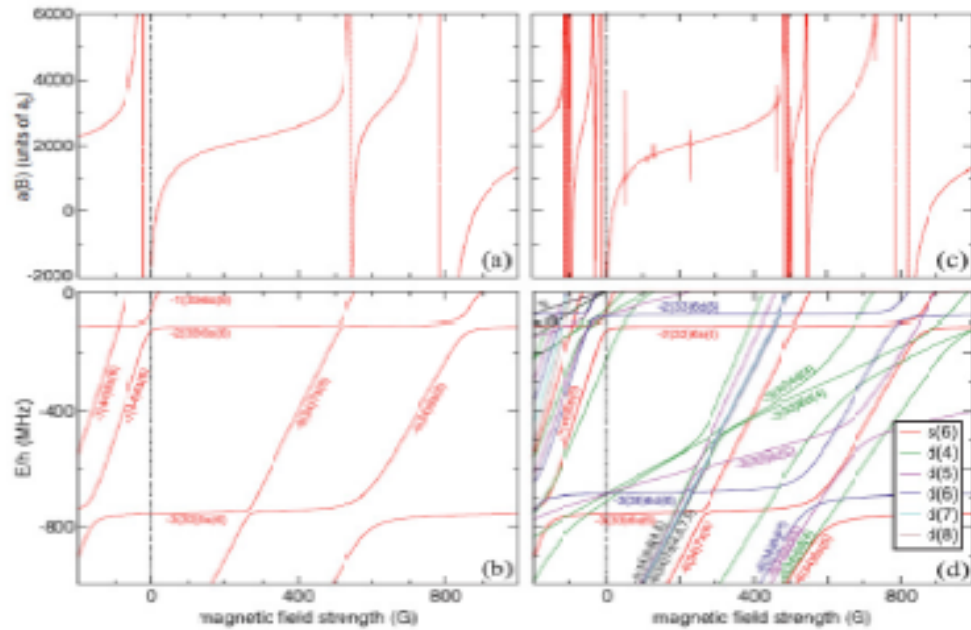


FIG. 1. (Color online) Molecular potential energy curves  $V_0(R)$  and  $V_1(R)$  for the single- and triplet states of  $\text{Cs}_2$ . The inset shows an expanded view of the long-range potentials separating to the two different  $f = 3$  and  $4$  hyperfine states of the atoms at magnetic field  $B = 0$ .



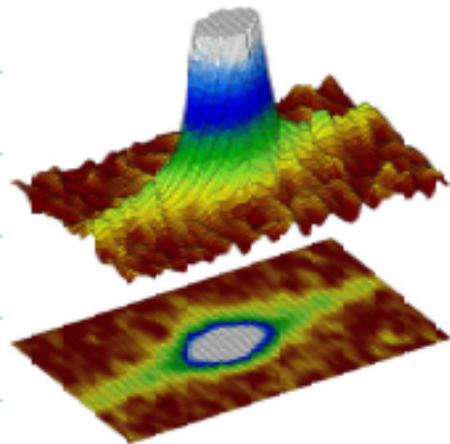
Example of the excellent agreement achieved in this Cs-Cs study, between the theoretical model (solid curve) and experimental measurements of bound state energies.

We will see some remarkable properties of the cold atoms enabled by having CONTROLLABLE INTERACTIONS

# An example from many-body BEC physics: The BOSENOVA

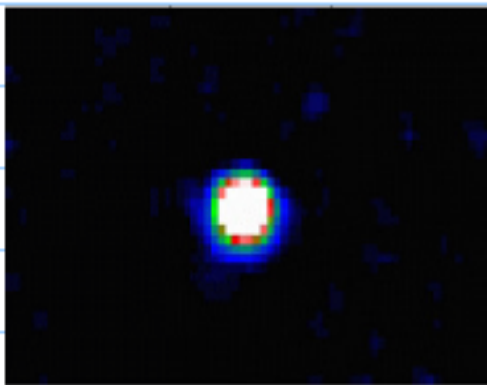
Recall the mean-field  
BEC equation (GP-equation):

$$H_0\psi(\vec{x}) + (N-1)\frac{4\pi\hbar^2 a_{sc}}{M}|\psi(\vec{x})|^2\psi(\vec{x}) = \epsilon\psi(\vec{x})$$



=> Note that for  $a_{sc} < 0$   
the system of  $N$  atoms  
has attraction and the  
atom cloud implodes and  
then explodes like a tiny  
SUPERNOVA

<https://www.nist.gov/news-events/news/2001/03/implosion-and-explosion-bose-einstein-condensate-bosenova>



The idea here is that a BEC of 85Rb atoms is first prepared with around 50,000 atoms, using a small positive scattering length. Then the magnetic field is used to tune the scattering length to a large negative value, causing the BEC to implode and shrink onto itself, at which point recombination processes ignite and release tremendous energy. This causes the BEC to explode like a supernova.

This scattering length control also enables  
the production of bizarre few-body states!  
We will see these later in this lecture.



## Confinement-induced resonances in a quasi-one-dimensional geometry

Consider collisions between two atoms confined to a cigar-shaped cylindrically-symmetric harmonic oscillator trap, which have a 3D scattering length  $a(E)$ . Ol'shanii(1998 PRL) showed that the interactions can be modeled as an effective 1D potential  $V_{\text{eff}}(z) = g \delta(z)$ ,

$$g_{1D} = \frac{\hbar^2}{\mu a_{\perp}} \frac{2a_s(E)}{a_{\perp} + c_1 a_s(E)}$$

$$c_1(k) = \zeta\left(\frac{1}{2}, 1 - \frac{1}{4}(ka_{\perp})^2\right)$$

$a_{\perp}$  is the oscillator length in the transverse dimension

**Mathematical curiosity:** Ol'shanii's derivation involves "regularization" of a divergent sum that arises, and re-expression as a Hurwitz zeta function that can be analytically continued to give finite answers. This is analogous to the famous "resummation" of the divergent series,

$$1+2+3+4+5+\dots = -1/12$$

**Numerical tests (and experiments) confirm the validity of this result.**

Application of this controllable "1D" effective interaction via a confinement-induced resonance resulted in the observation of the predicted 1D quantum degenerate gas, usually called the "Tonks-Girardeau gas", by at least 2 groups in 2004:

### Tonks-Girardeau gas of ultracold atoms in an optical lattice

Nature 2004

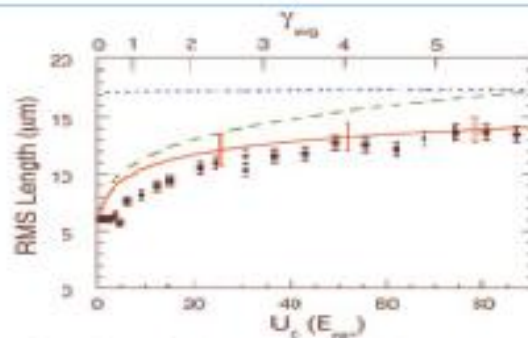
Belén Paredes<sup>1</sup>, Artur Widera<sup>1,2,3</sup>, Valentin Murg<sup>1</sup>, Olaf Mandel<sup>1,2,3</sup>,  
Simon Fölling<sup>1,2,3</sup>, Ignacio Cirac<sup>1</sup>, Gora V. Shlyapnikov<sup>1</sup>,  
Theodor W. Hänsch<sup>1,2</sup> & Immanuel Bloch<sup>1,2,3</sup>

### Observation of a One-Dimensional Tonks-Girardeau Gas

Science 2004

Toshiya Kinoshita, Trevor Wenger, David S. Weiss\*

Fig. 8. Plot of the rms full length of the 1D atom cloud versus the transverse confinement at  $P = 12$  nW. The circles represent the measured values, with the instrumental resolution deconvolved [see text]. Error bars on the experimental points reflect residual trap excitations that arise when the lattice is turned on. The curves for TG theory (short-dashed line), mean field theory (long-dashed line), and exact 1D free gas theory (solid line) are shown [7]. Error bars on the theory curve reflect uncertainties in experimental parameters and are dominated by a 5% uncertainty in  $\psi_{\perp}$ . With no free parameters, the data conform to the exact theory [7] above  $U_{\perp} \approx 29 E_{\text{rec}}$ , where the system is purely 1D.

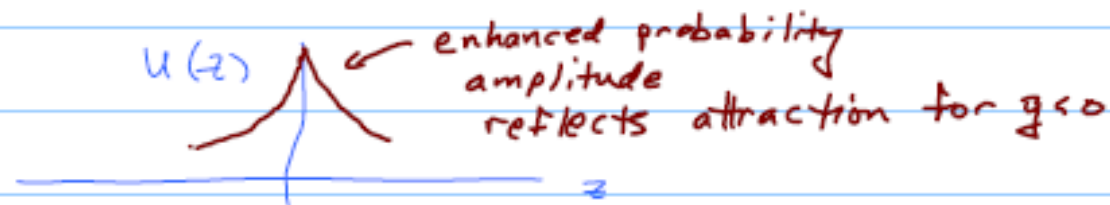


# A surprising result about bosons in 1-Dimension with a strong repulsion: FERMIONIZATION

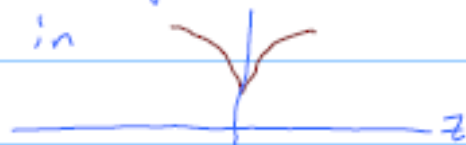
- i.e. the bosons can behave like fermions!

Why? Consider 2 identical bosons in 1D with interaction potential  $V(z) = g \delta(z)$

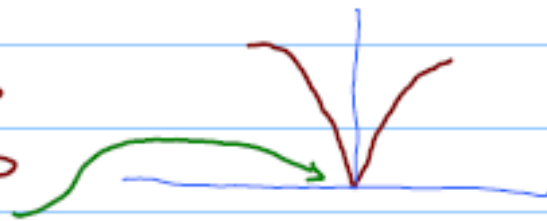
When  $g < 0$  and the bosons attract each other, their wave function near  $z=0$  looks like:



But if  $g > 0 \Rightarrow$  REPULSION, the  $z=0$  amplitude is suppressed, as in



and if  $g \rightarrow +\infty$   
 $U(z) \rightarrow 0$   
 $z \rightarrow 0$

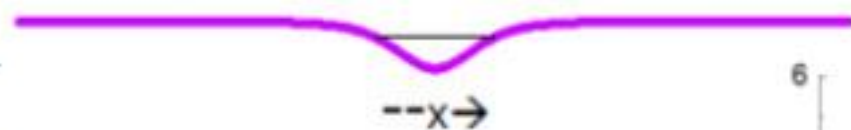


Consequence: The strongly repelling bosons have a wave function  $\Psi = |\det U_n(z_m)|$  whose square agrees with NON-INTERACTING FERMIONS!

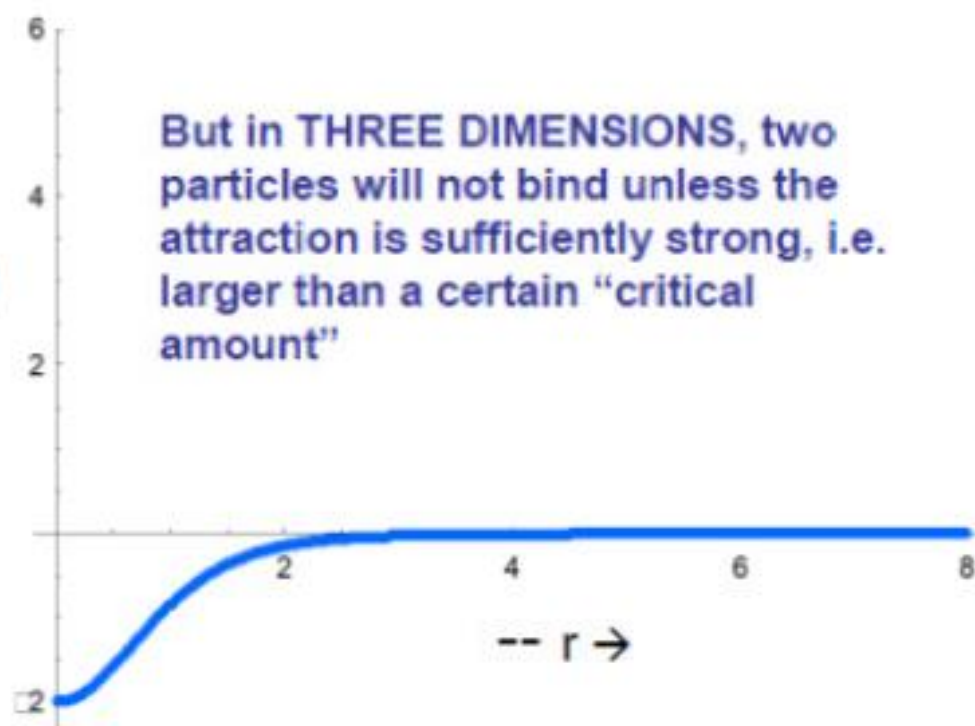
## Introduction to the Efimov Effect – Preliminary considerations for 2 particles

Start with 2-body quantum  
physics – in ONE DIMENSION,  
any attraction however small is  
enough to create a bound state.

$V(x)$  versus  $x$



$V(r)$



But in THREE DIMENSIONS, two  
particles will not bind unless the  
attraction is sufficiently strong, i.e.  
larger than a certain "critical  
amount"

## (2) Universal Efimov physics (3 identical bosons in 3D)

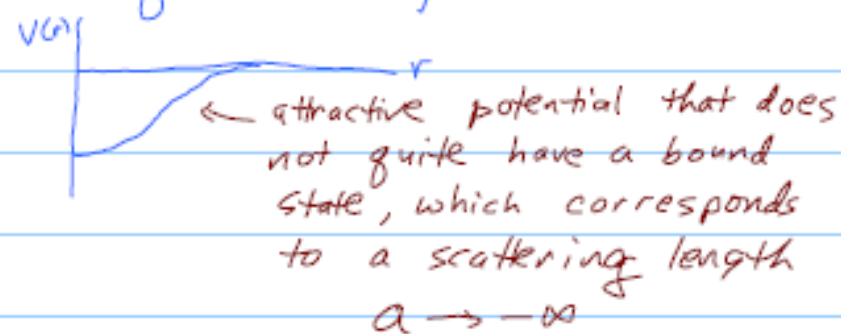
- zero range theory

Efimov Physics: a review by P Naidon, S Endo  
Reports on Progress in Physics 80 (5), 056001 2017

- van der Waals universality

### The Efimov effect - Basic idea for the $A+A+A$ system

Consider 3 identical bosons that attract each other, in 3D,  
but the attraction is not quite strong enough to bind  
two atoms together



Vitaly Efimov's 1970 prediction:

For 3 particles having this pairwise interaction, i.e.  $\hat{V}_{tot} = V(r_{12}) + V(r_{23}) + V(r_{31})$ ,

the TRIMER system  $A_3$

has an INFINITE Number of bound states

given as a geometric series of levels

$$E_{n+1} = E_n e^{-2\pi/s_0} \quad \text{where } s_0 \approx 1.0062\dots$$

$n = 1, 2, 3, \dots \infty$

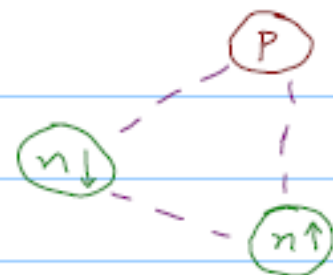
is a universal constant  
and  $e^{2\pi/s_0} \approx 22.7^2 = 515$

← Start  
from 2-body  
interactions



Efimov's original study was for the 3-nucleon system  $pnn$ , the TRITON.

Even though  $p+n_d+n_r$  is obviously NOT 3-identical bosons, the analogy is appropriate because



(1) The 2 neutrons are in different spin substates and therefore in a sense "distinguishable"

and

(2) The scattering lengths are much larger than the range  $r_0 \sim 1 \text{ fm}$  of the nuclear forces

Efimov suggested that the triton might be viewed as an Efimov state, since  $n-p-n$  has large, 2-body scattering lengths, namely the neutron-proton scattering lengths

$A(n-p) = -24 \text{ fm}$  (singlet),  $5.4 \text{ fm}$  (triplet)

and a large negative neutron-neutron scattering length,

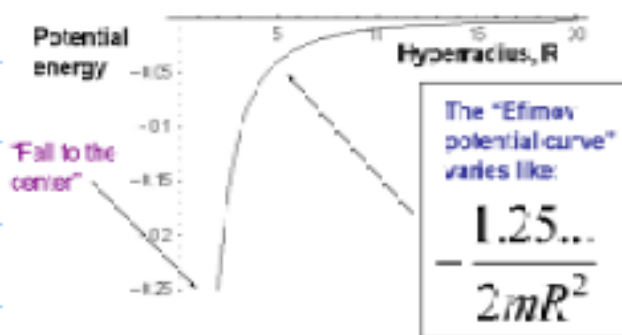
$A(n-n) = -19 \text{ fm}$  (singlet) (taken from Trotter, Tomow, et al., nucl-ex/9904011)

And the range of the nuclear interaction is about  $r_0 = 1 \text{ fm}$ .

Whereas the expected "number of Efimov states" is

$$N \approx \frac{1}{\pi} \ln\left(\frac{|a|}{r_0}\right) \approx 0.9 - 1.0$$

To understand this quantitatively, look at Efimov's effective potential energy curve as a function of the hyperradius:



Mathematical Detail. Once you have this "effective dipole-type attractive potential curve", it is TRIVIAL!

By definition, "trivial" means that it can be found in Landau and Lifshitz's book on quantum mechanics. Specifically, the solutions are simply Bessel functions ( $p^2$  imaginary order, and imaginary argument).

Our interest was picqued in the 1990s after Joe Macek showed that the adiabatic hyperspherical representation is an effect way to rederive Efimov's result in the context of a ZERO RANGE model.

But with my PhD student Brett Esry and other collaborators, we tested whether the Efimov effect survives even for extended (but finite) range 2-body interaction potentials.

And we found that it did survive: there is a **universal behavior** even for large but finite  $|A|$  which differs qualitatively for positive versus negative  $A$ .

**References to our early papers calculating the problem from an adiabatic hyperspherical viewpoint:**

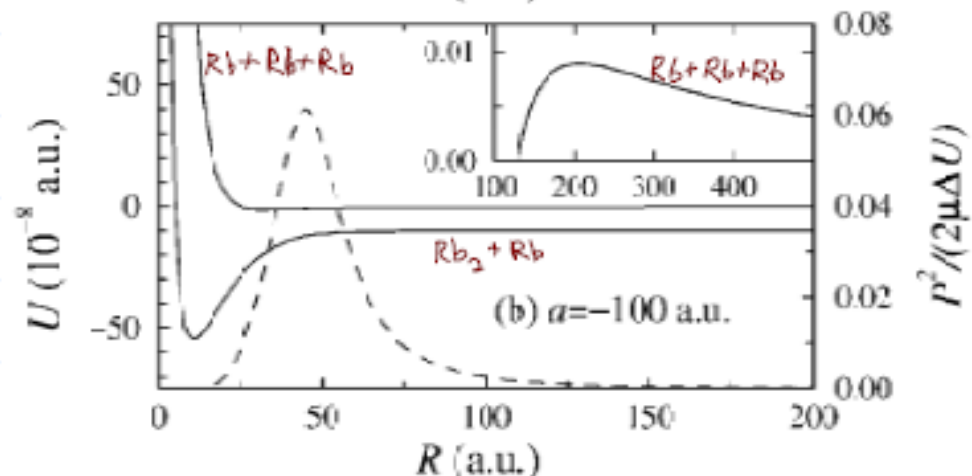
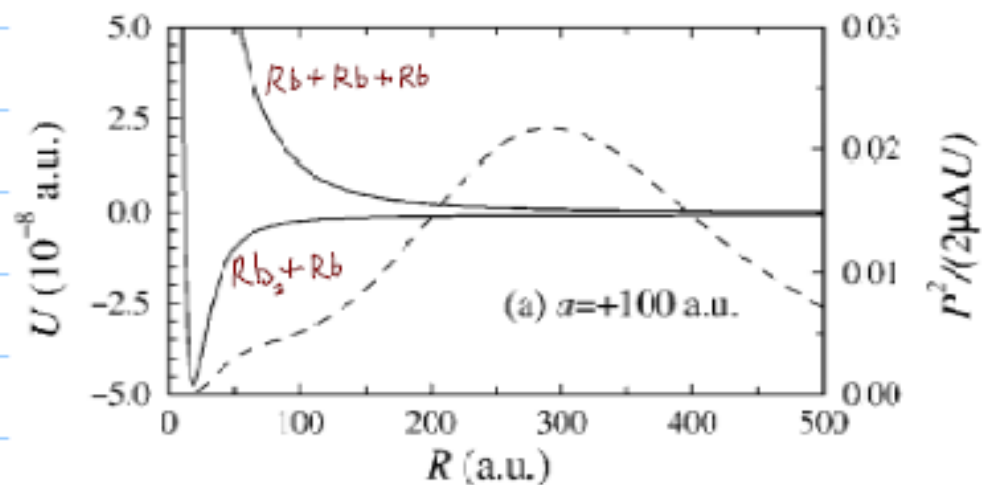
->Esry et al., J. Phys. B: At. Mol. Opt. Phys. **29** (1996) L51-L57

->Esry et al., Phys. Rev. Lett. **83**, 1751 (1999)

->and at almost the same time Nielsen and Macek published some similar results and reached some overlapping conclusions (in a zero-range model) in PRL **83**, 1566 (1999).

Through our numerical studies, we found that there is a universal behavior at positive  $A$ , namely there is a fully repulsive 3-body entrance channel and a high-lying recombination channel representing (dimer+atom)

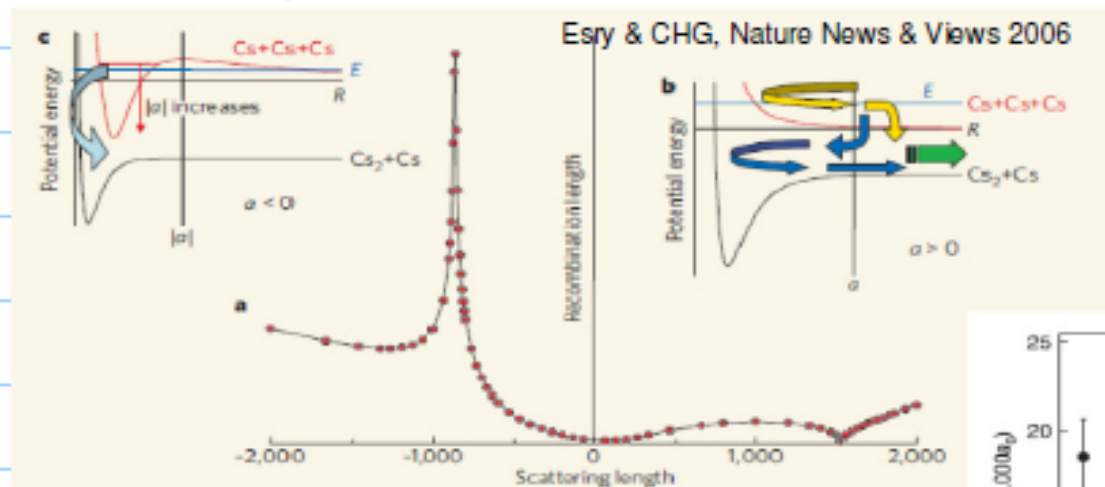
Whereas there is also a universal but VERY DIFFERENT behavior at negative  $A$ , namely there is a partially repulsive 3-body entrance channel but with a potential barrier that can support shape resonances, and only deep recombination channels representing ("deeply bound dimer" + atom)



After carrying out coupled channel calculations, including the nonadiabatic coupling of these channels, we found the following universal behavior of recombination rates of 3 equal mass particles (either identical bosons or distinguishable particles) as a function of the two-body scattering length.

At ( $a < 0$ ) the potential barrier supports a shape resonance at certain energies or certain values of the scattering length  $a$ , and there are an infinite series of these EFIMOV resonances (at  $a < 0$ ), separated by the universal Efimov scaling factor 22.7, recombining into deep dimers, shown

At ( $a > 0$ ) there is no potential barrier supporting shape resonances (Efimov resonances) at all! But at certain values of the scattering length  $a$  there are a series of Stueckelberg interference MINIMA, in the recombination rate into deep dimers, also separated by the Efimov scaling factor 22.7, via the pathways shown below



### Evidence for Efimov quantum states in an ultracold gas of caesium atoms

NATURE Vol 440 | 16 March 2006

T. Kraemer<sup>1</sup>, M. Mark<sup>1</sup>, P. Waldburger<sup>1</sup>, J. G. Dand<sup>1</sup>, C. Chin<sup>1,2</sup>, B. Engeser<sup>1</sup>, A. D. Lange<sup>1</sup>, K. Pilch<sup>1</sup>, A. Jaakkola<sup>1</sup>, H.-C. Nägerl<sup>1</sup> & R. Grimm<sup>1,2</sup>

Congratulations, Rudi Grimm, for earning a share of the Foddeev Medal, for this experimental demonstration of Efimov physics!

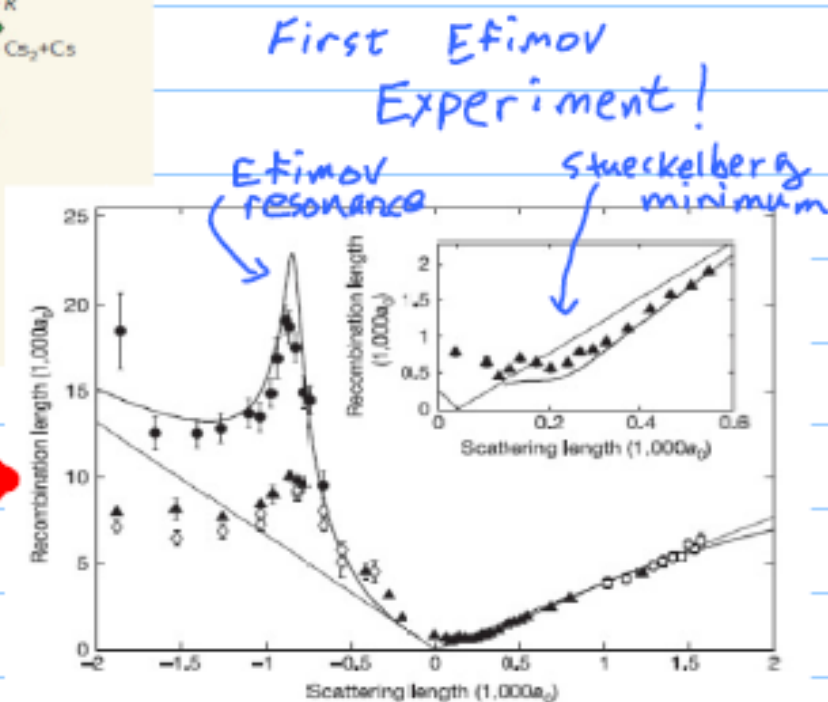


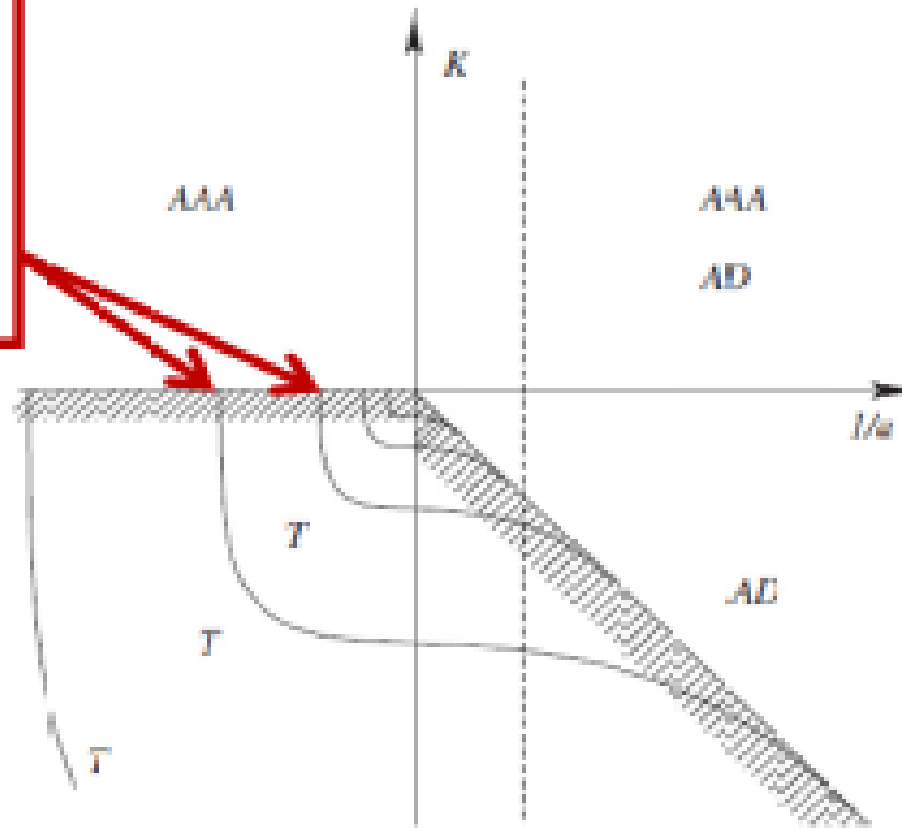
Figure 2 | Observation of the Efimov resonance in measurements of three-body recombination. The recombination length  $\rho_3 \propto L_3^{1/4}$  is plotted as a function of the scattering length  $a$ . The dots and the filled triangles show the experimental data from set-up A for initial temperatures around 10 nK and 200 nK, respectively. The open diamonds are from set-up B at

The full spectrum of universal Efimov levels near unitarity, where the scattering length ( $|a|$ ) is much larger than the

## Infinite ladder of 3-body energy levels (sqrt) versus $1/a$

*E. Braaten, H.-W. Hammer / Physics Reports-428 (2006) 259–300*

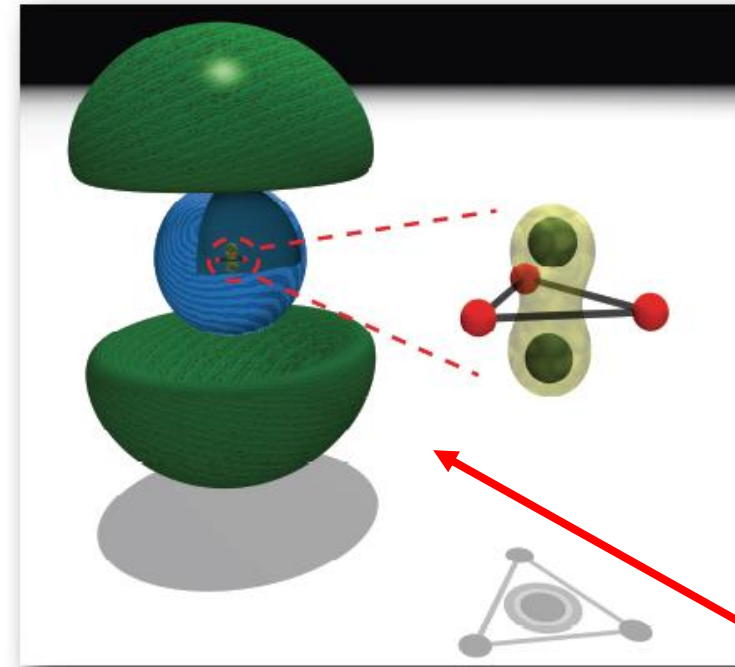
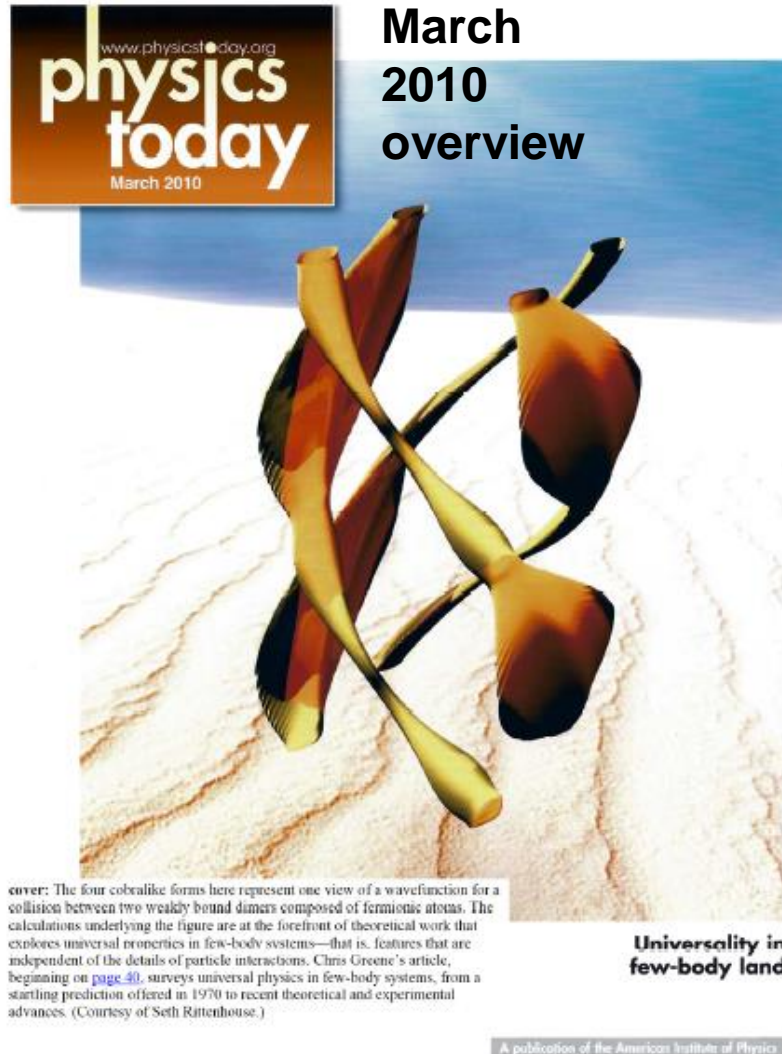
Efimov resonances observable in 3-body recombination in an ultracold gas





# N-Body Recombination and the Efimov effect

Chris Greene, with Jose D’Incao, Nirav Mehta, Seth Rittenhouse (at ICAP) and Javier von Stecher, JILA and Physics, U. of Colorado-Boulder



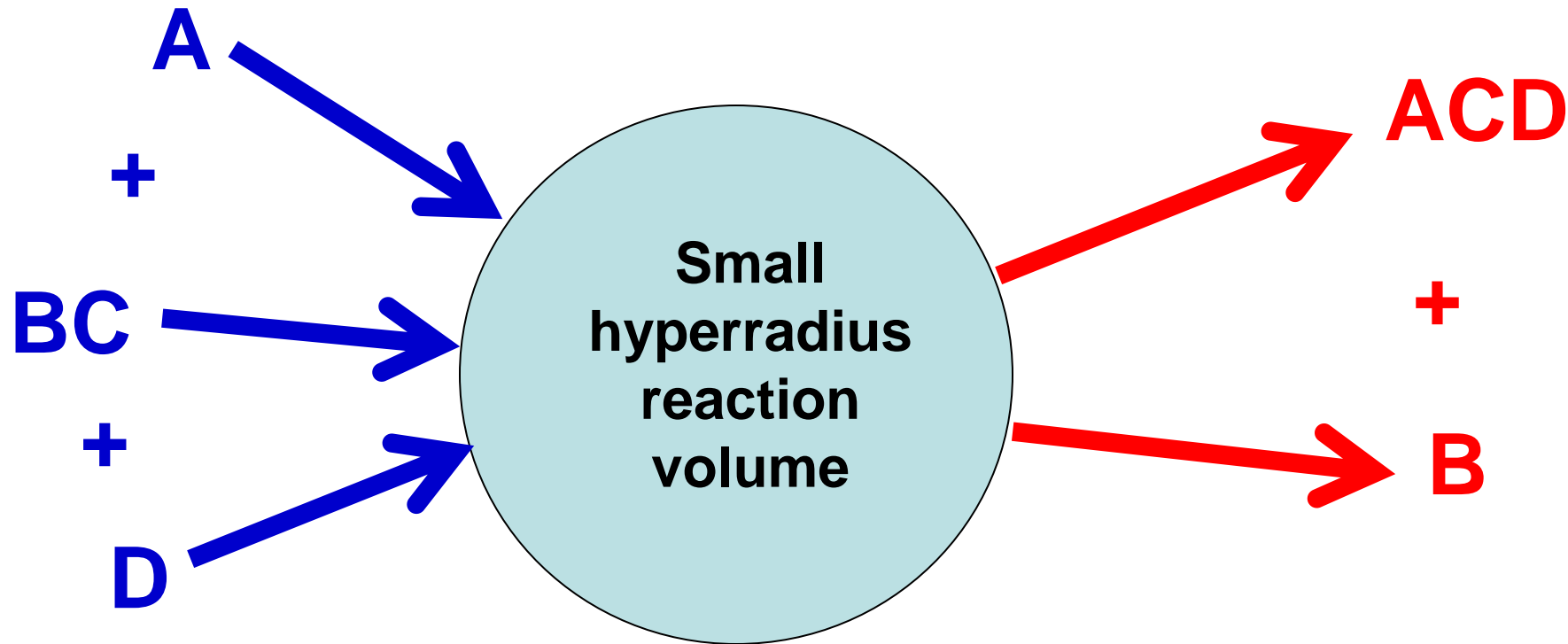
**Depicted:**  
**A big universal molecule with 4 atoms, “attached” to a 3-body Efimov state**

**•Thanks, NSF!**



Ugo Fano's vision around 1981, following a promising line of research dating back to earlier work by:

Delves, Smirnov, Macek, Lin, Schatz, Kuppermann, ...



→ All reactive processes can be viewed as a single coordinate, the hyperradius  $R$ , evolves from large to small and then to large values again

**Our main theoretical tool:  
formulate the problem in  
hyperspherical coordinates,  
treating the hyperradius R  
adiabatically**

The hyperradius R (squared) is a coordinate proportional to total moment of inertia of any N-particle system, i.e.:

$$R^2 = \frac{1}{M} \sum_i m_i r_i^2 \quad \text{also } \rho^2$$

Here  $r_i$  is the distance of the i-th particle from the center-of-mass. All other coordinates of the system are 3N-4 hyperangles.

And then the rest of the problem comes down to calculating energy levels as a function of R, which we call “hyperspherical potential curves”, and their mutual couplings, which can then be used to compute bound state and resonance properties, scattering and photoabsorption behavior, nonperturbatively

This follows the formulation of the N-body problem in the adiabatic hyperspherical representation, as pioneered by Macek, Fano, Lin, Klar, and others



Strategy of the adiabatic hyperspherical representation: **FOR ANY NUMBER OF PARTICLES**, convert the partial differential Schroedinger equation into an infinite set of coupled **ordinary** differential equations:

To solve:

$$\left[ -\frac{1}{2\mu} \frac{\partial^2}{\partial R^2} + \frac{\Lambda^2}{2\mu R^2} + V(R, \theta, \varphi) \right] \psi_E = E \psi_E$$

First solve the fixed-R Schroedinger equation, for eigenvalues  $U_n(R)$ :

$$\left[ \frac{\Lambda^2}{2\mu R^2} + \frac{15}{8\mu R^2} + V(R, \theta, \varphi) \right] \Phi_\nu(R; \Omega) = U_\nu(R) \Phi_\nu(R; \Omega)$$

Next expand the desired solution into the complete set of eigenfunctions with unknowns  $F(R)$

$$\psi_E(R, \Omega) = \sum_\nu F_{\nu E}(R) \Phi_\nu(R; \Omega)$$

And the original T.I.S.Eqn. is transformed into the following set which can be truncated on physical grounds, with the eigenvalues interpretable as adiabatic potential curves, in the Born-Oppenheimer sense.

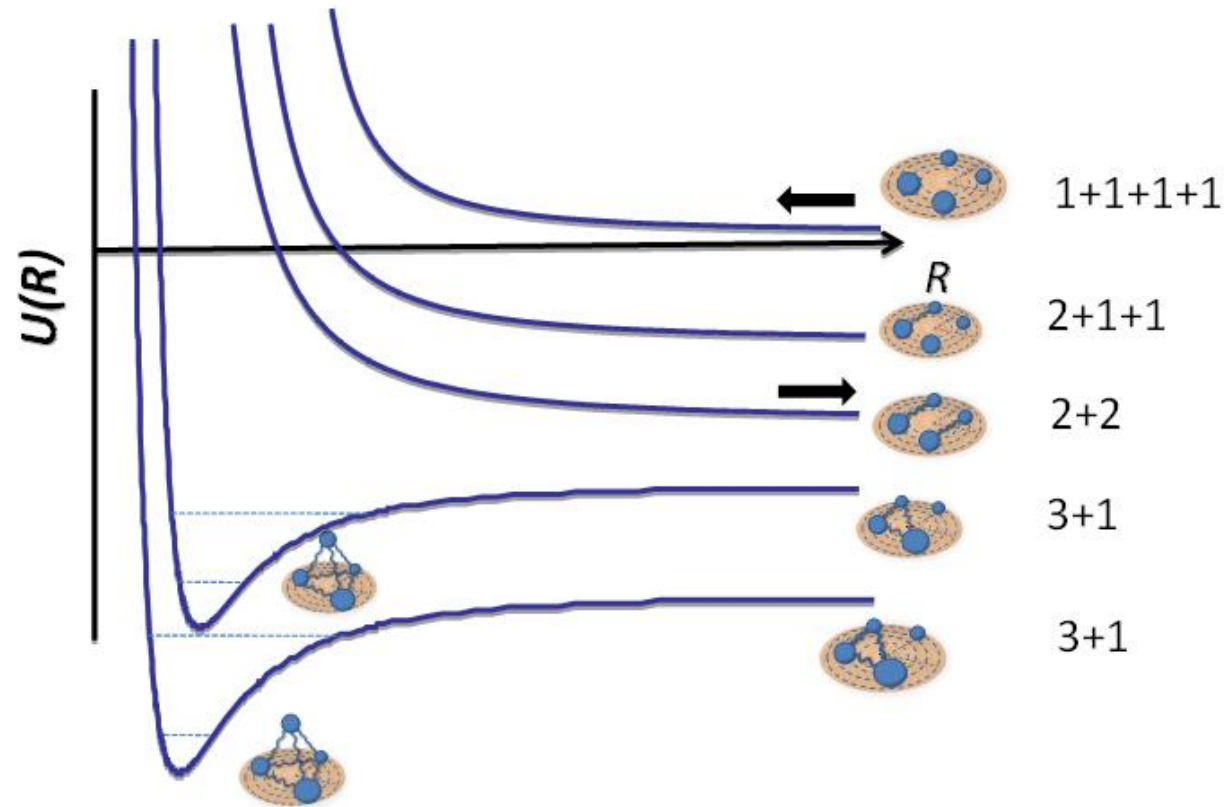
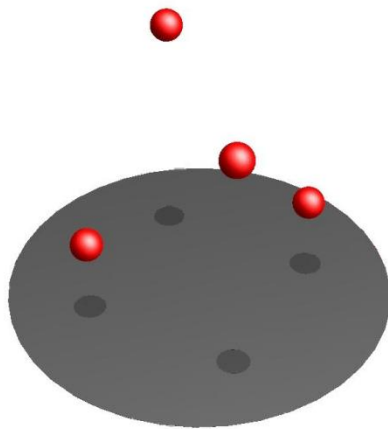
$$\left[ -\frac{1}{2\mu} \frac{d^2}{dR^2} + U_\nu(R) \right] F_{\nu E}(R) - \frac{1}{2\mu} \sum_{\nu'} \left[ 2P_{\nu\nu'}(R) \frac{d}{dR} + Q_{\nu\nu'}(R) \right] F_{\nu' E}(R) = E F_{\nu E}(R)$$



## Hyperspherical Picture of 4-body recombination

... think Born Oppenheimer

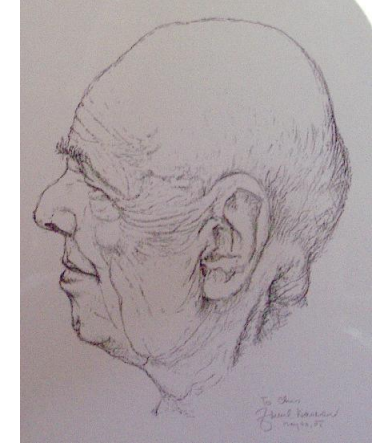
Fragmentation  
thresholds



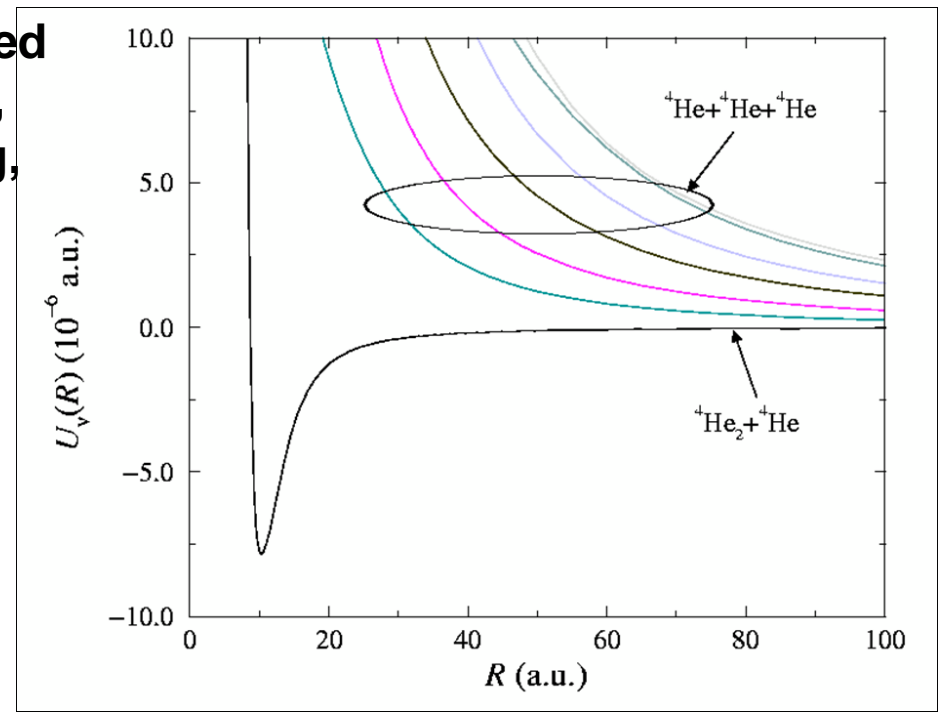
# Elements of Fano's Vision

1. The vital role of eigenmodes of the most relevant operators in any given problem, usually including all or part of the Hamiltonian
2. The transformative importance of a *picture*, to help see pathways and mechanisms, as in the Born-Oppenheimer potential curves for reactive processes in chemistry
3. Qualitative insight can often be extracted powerfully from semiclassical pictures, as in WKB, Landau-Zener-Stueckelberg, etc.

**J=0 adiabatic hyperspherical potential curves for He+He+He (with Suno, Esry, & Burke, 2002 PRA)**



Ugo Fano, sketched by Zdenek Herman



## Various strategies for getting the potential curves:

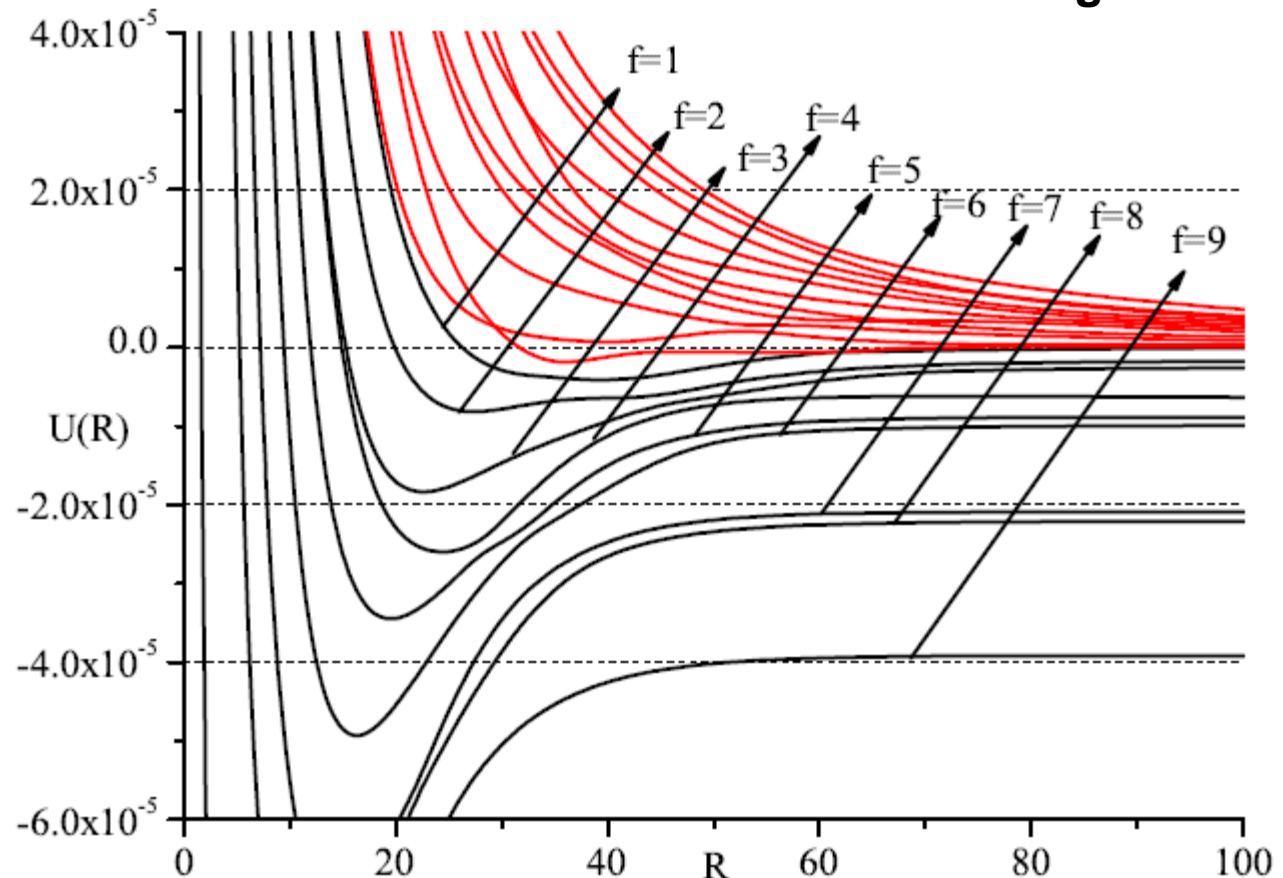
Expand the adiabatic eigenfunction into a local basis in the hyperangles, such as B-splines, finite elements, DVR, etc. For example, for the 3-body problem, this leads to a two dimensional eigenproblem to be solved at each hyperradius, typically  $100 \times 100 = 10^4$  total basis functions

See e.g. Zhou,  
Lin, & Shertzer, J  
Phys B 1993

Esry, Lin, CHG  
1996 PRA

This method is  
very accurate for  
3 bodies with  
arbitrary  
interactions, but  
difficult to extend  
to  $N > 3$ .

2011 J. Wang & CHG



Three body resonances predicted in recombination, studied at near zero energy as a function of scattering length which can be controlled by a magnetic field.

J. Phys. B: At. Mol. Opt. Phys. 42 (2009) 044016

# The short-range three-body phase and other issues impacting the observation of Efimov physics in ultracold quantum gases

D’Incao, Esry, CHG

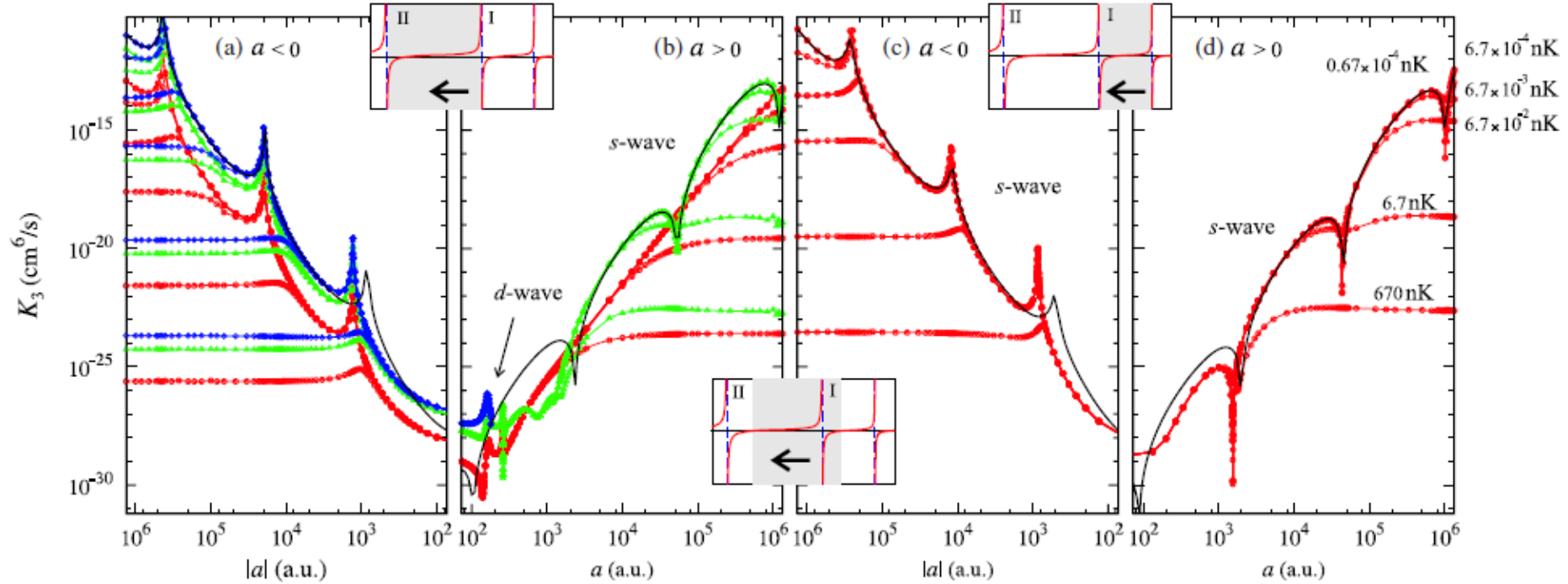
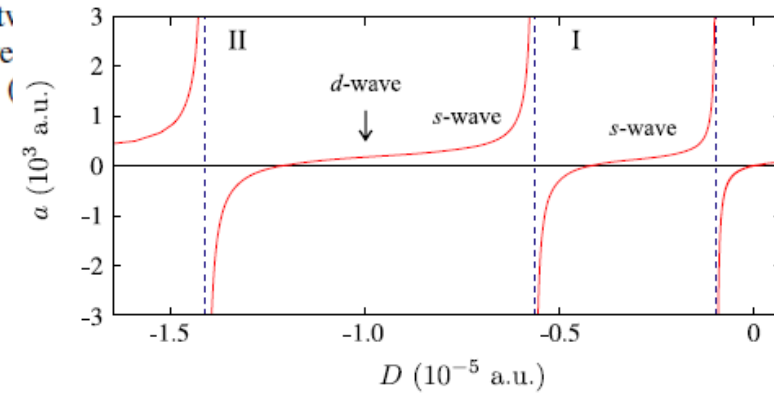
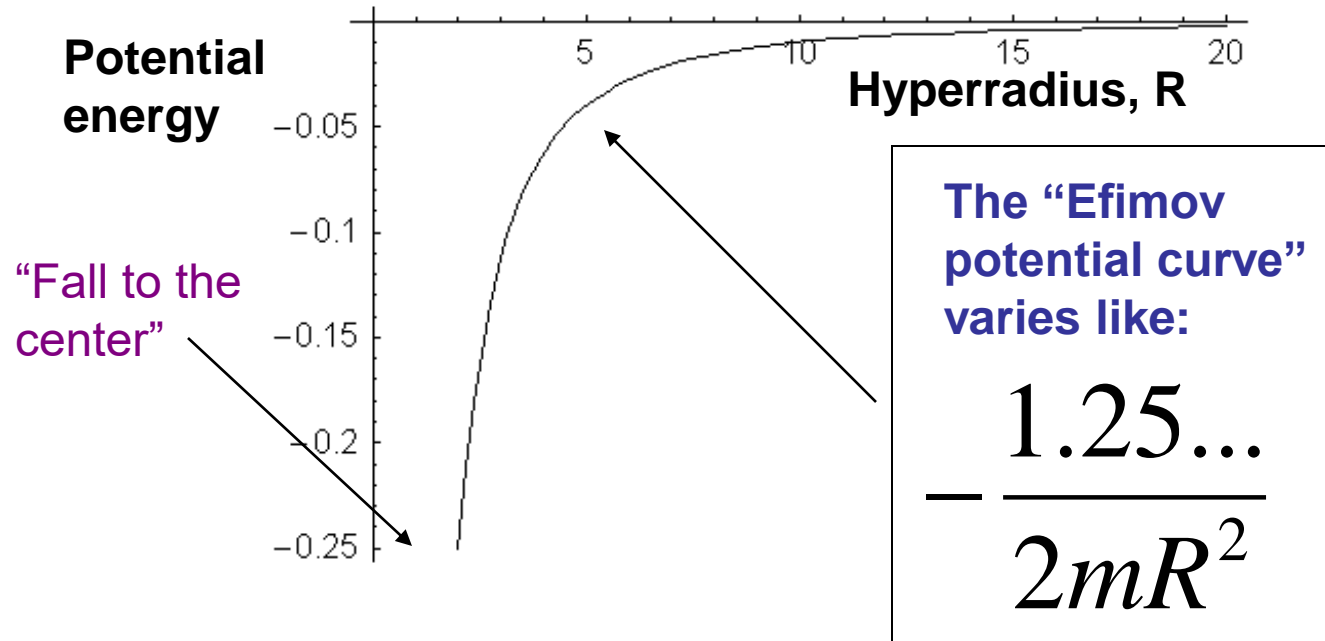


Figure 3. Recombination rate for  $a$  covering regimes with different numbers of  $\nu$  (b) recombination has contributions from the deeply (red circles) and weakly (green diamonds) bound states. The lines without symbols are the fit of equations (1) and (2).

$$K_3 = \frac{4590 \sinh(2\eta_P)}{\sin^2[s_0 \ln(|a|/r_0) + \Phi_P] + \sinh^2 \eta_P} \frac{\hbar |a|^4}{m}$$



To understand the Efimov effect, look at the effective potential energy curve at unitarity, as a function of the hyperradius:



**Mathematical Detail.** Once you have this “effective dipole-type attractive potential curve”, the rest is ‘TRIVIAL’!

Here, ‘trivial’ means that the solutions are simply Bessel functions (of imaginary *order*, and imaginary *argument*).

$$E_{n+1} = E_n e^{-2\pi/s_0}, \text{ where } s_0 = 1.00624\dots \text{ is a universal constant.}$$



# **A flurry of Efimov physics experiments in 2008-9:**

## **BOSONS**

- 1. Zaccanti, Inguscio, Modugno et al. Nature Phys. 5, 586 (2009)**
- 2. Barontini, Thalhammer, Inguscio, Minardi, et al. PRL 103, 043201 (2009)**
- 3. Gross, Shotan, Kokkelmans, Khaykovich, PRL103, 163202 (2009)**
- 4. Pollack, Dries, Hulet, Science 326, 1683 (2009)**
- 5. Knoop, Ferlaino, Nagerl, Grimm, et al. Nature Phys. 5, 227 ('09)**

## **DISTINGUISHABLE FERMIONS**

- 6. Ottenstein, Lompe, Kohnen, Wenz, Jochim, PRL 101, 203202 (2008)**
- 7. Huckans, Williams, O'Hara et al, PRL 102, 165302 (2009)**
- 8. Williams, Huckans, O'Hara et al. PRL 103, 130404 ('09)**

# Observation of an Efimov spectrum in an atomic system

NATURE PHYSICS | VOL 5 | AUGUST 2009

586

M. Zaccanti<sup>1\*</sup>, B. Deissler<sup>1</sup>, C. D'Errico<sup>1</sup>, M. Fattori<sup>1,2</sup>, M. Jona-Lasinio<sup>1</sup>, S. Müller<sup>3</sup>, G. Roati<sup>1</sup>, M. Inguscio<sup>1</sup> and G. Modugno<sup>1</sup>

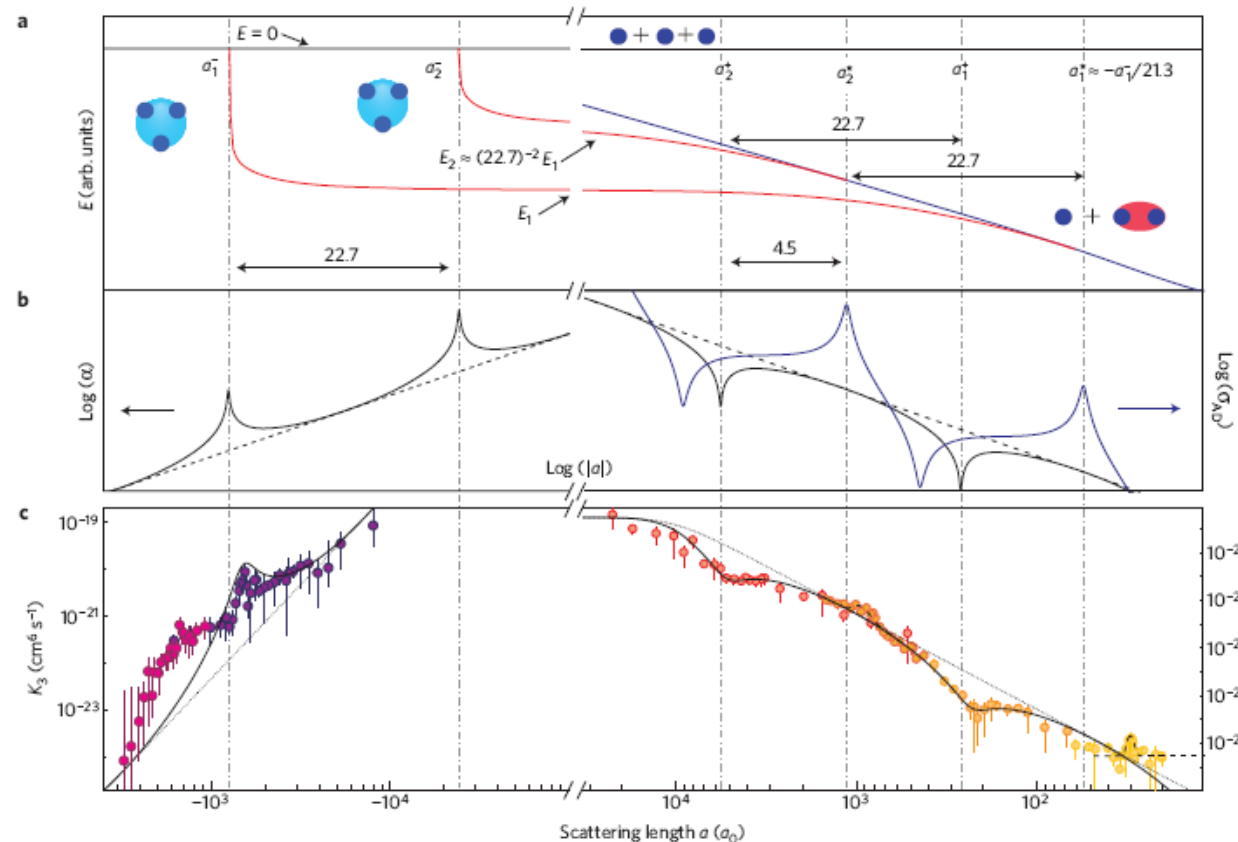


**Figure 1 | Efimov spectrum.** **a** Theoretical binding energy of two consecutive Efimov states (red) and of the dimer state (blue) in the universal regime versus the scattering length  $a$ . **b**, Theoretical three-body recombination rate  $\alpha$  (black) and atom-dimer elastic cross-section  $\alpha_{AD}$  (blue). The vertical dash-dotted lines indicate the position of the detectable maxima and minima in the three-body observables, for which the relevant scaling rules are summarized in **a**. The dashed lines indicate the  $a^4$  behaviour of the three-body recombination rate expected in the absence of Efimov states. **c**, Measured recombination coefficient  $K_3$  in an ultracold potassium gas (circles), featuring deviations from the bare  $a^4$  trend (dotted line), and fitted behaviour assuming a local universal trend for  $K_3$  in the vicinity of the two recombination minima at  $a > 0$  and of the Efimov resonance at  $a < 0$  (solid line), see text. The other two features due to the atom-dimer resonances  $a_1^+$  and  $a_2^+$ , not expected by theory, are locally fitted with a Gaussian profile superimposed to a constant background and to the universal behaviour, respectively (dashed lines). The various colours correspond to different data sets. For all data points, the error bars are the root sum squared of the standard error of the mean value resulting from the fit and of the uncertainty on the trap frequencies (see the Methods section).

**Nielsen and Macek, 1999 PRL; Esry, Greene, and Burke, 1999 PRL-3-body recombination at large  $a$  from an adiabatic hyperspherical perspective**

**Other groups subsequently rederived the Efimov physics in the universality regime of large two-body scattering lengths, especially relevant for 3-body recombination, using other methods:**

**Braaten and Hammer, 2000-2006 – Effective field theory approach**

**Shepard, 2007 – Fadeev treatment in momentum space, effective theory**

**Lee, Köhler, Julienne, 2007 – 3-body Green's function approach based on a transition matrix; basic formulation was developed in nuclear physics by Sandhas, Alt, and Grassman.**

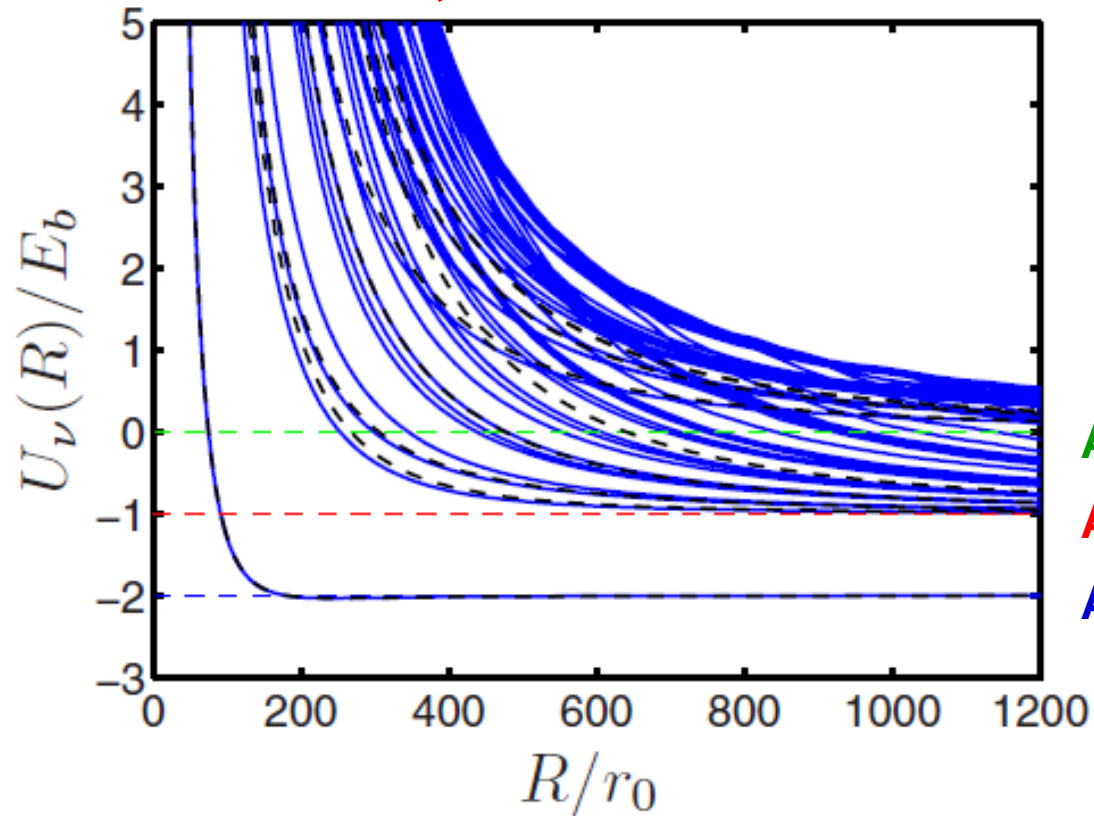
**Gogolin, Mora, Egger, 2008 – Analytic solution of a model**

**Floerchinger, Schmidt, Moroz, Wetterich, 2009 – functional renormalization approach**

## How to go beyond 3 particles:

### Correlated Gaussian Hyperspherical Method

von Stecher & CHG, PRA 2009

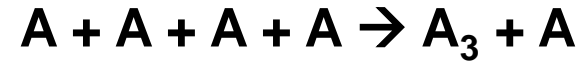


Computed potential energy curves:  
Energy versus hyperradius for a 4-atom  
system

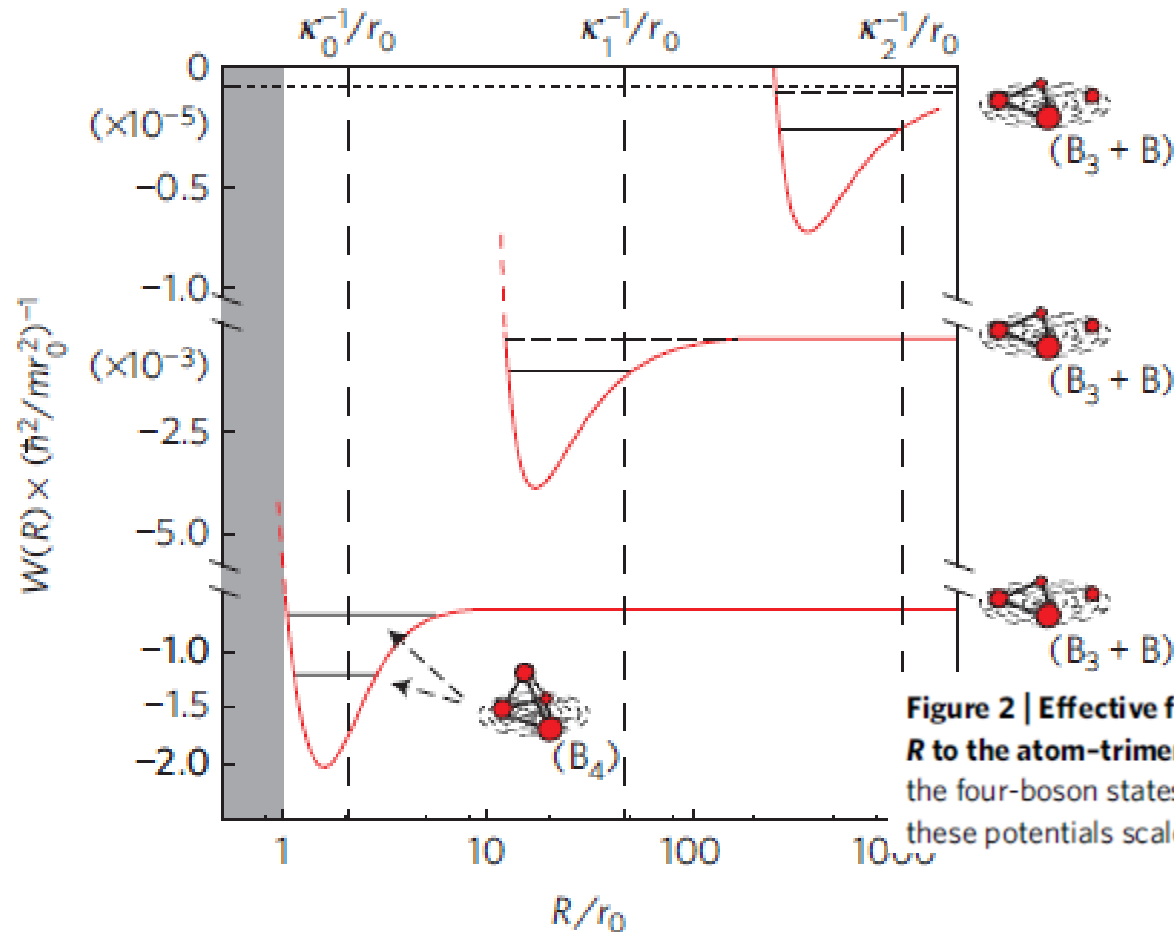
FIG. 1. (Color online) Adiabatic hyperspherical potential curves  $U_\nu(R)$  (solid lines) for two spin-up and two spin-down fermions with an atom-atom scattering length  $a_s=100r_0$ . The dashed line at  $E=2E_b$  (blue) is the dimer-dimer threshold, the dashed line at  $E=E_b$  (red) is the dimer-two-atom threshold, and the dashed line at  $E=0$  (green) is the four-atom threshold. Dashed curves are predictions from Ref. [24].

## Applications

- Theory (**Mehta et al., PRL 103, 153201 (2009)**) of N-body recombination processes, e.g.



- The 4-boson system: 4-body recombination and its surprising importance



von Stecher,  
D’Incao, & CHG,  
Nature Phys. 2009

D’Incao, von  
Stecher, & CHG,  
PRL 2009

Figure 2 | Effective four-boson potentials for  $|a| = \infty$  converging at large  $R$  to the atom-trimer thresholds. Solid and dashed black lines represent the four-boson states shown in Fig. 1a. The position in  $R$  of the minimum of these potentials scales with the size of the Efimov state, indicated in the

## Previous important studies of the 4-boson system in the universality regime in 3D:

Platter, L., Hammer, H. & Meißner, U. Four-boson system with short-range interactions. *Phys. Rev. A* 70, 52101 (2004).

- Hammer, H. W. & Platter, L. Universal properties of the four-body system with large scattering length. *Eur. Phys. J. A* 32, 113–120 (2007).

“We have conjectured, that there are always two four-body resonances between any two three-body states.” (i.e. below each Efimov state) + Also, no 4-body param.

---

Hanna, G. J. & Blume, D. Energetics and structural properties of three-dimensional bosonic clusters near threshold. *Phys. Rev. A* 74, 063604 (2006).

**...also found general correlations between N-body bound levels and (N-1)-body bound levels**

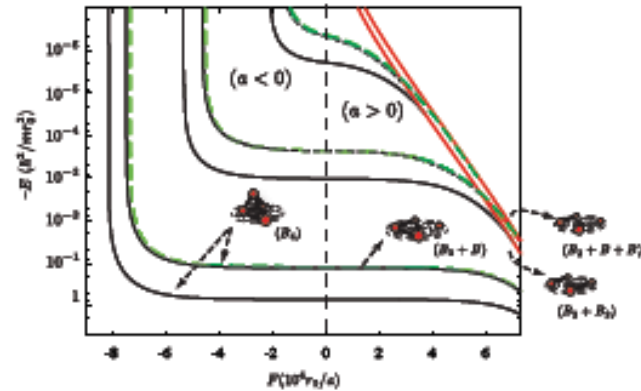
---

Yamashita, M. T., Tomio, L., Delfino, A. & Frederico, T. Four-boson scale near a Feshbach resonance. *Europhys. Lett.* 75, 555–561 (2006).

**...conclude that a “4-body parameter” is in fact needed, but they only studied low (non-universal states), which is presumably why they reach a different conclusion from that of Platter and Hammer and also different from ours.**



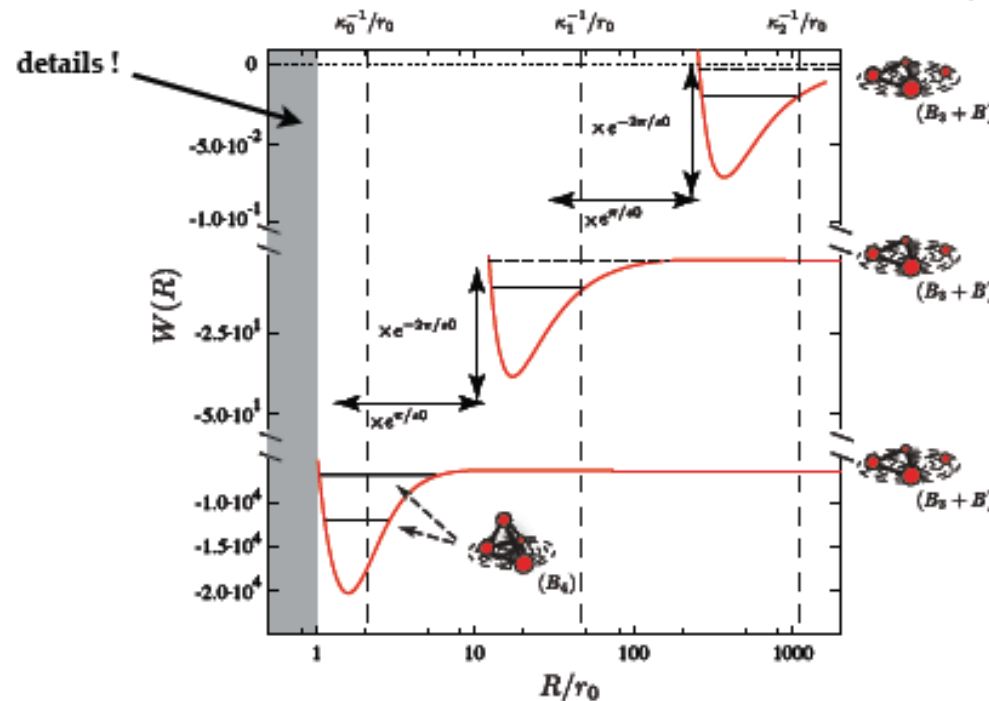
# Four-boson Spectrum



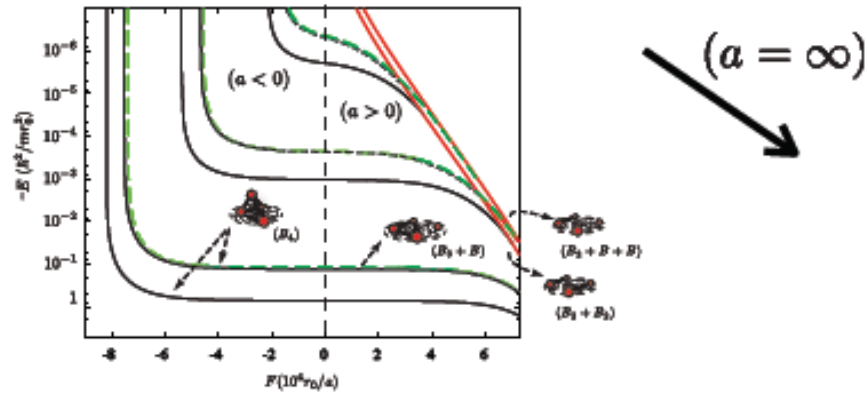
**Two four-body states per Efimov trimer !!!**

$$E_{4b}^{(n,m)} = c_m E_{3b}^{(n)} \quad \begin{array}{l} m = 1, 2 \\ n = 1, 2, \dots, \infty \end{array}$$

( $c_1 \approx 4.58$ ,  $c_2 \approx 1.01$ )  
(no four-body parameter)



**Four-body physics is truly Universal !!!**  
(geometric scaling: Efimov physics)



**Two four-body states per Efimov trimer !!!**

$$E_{4b}^{(n,m)} = c_m E_{3b}^{(n)} \quad \begin{array}{l} m = 1, 2 \\ n = 1, 2, \dots, \infty \end{array}$$

$$(c_1 \approx 4.58, c_2 \approx 1.01)$$

**(no four-body parameter)**

Our findings

## Controversy

**Hammer, Platter (2007)**

**VS**

**Yamasita et. al (2006)**

**(no four-body parameter)**

**(four-body parameter)**

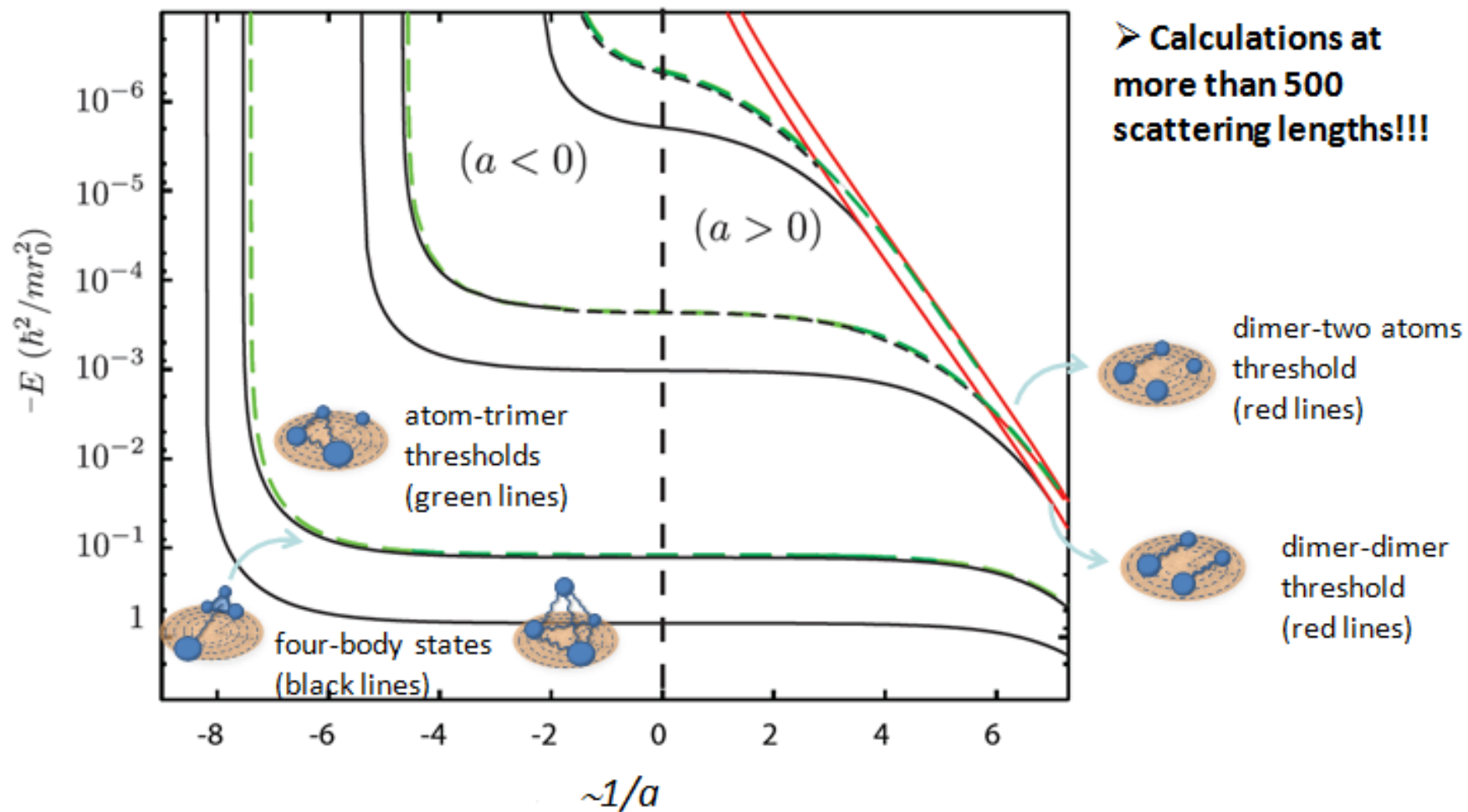
$$E_{4b}^{(0,2)} \approx 1.01 E_{3b}^{(0)}$$

$$E_{4b}^{(0,1)} \approx 5.0 E_{3b}^{(0)}$$

**Our results are consistent with Hammer & Platter's insightful conjecture, and also with Hanna & Blume's calculations**



## Spectrum: Extended Efimov plot



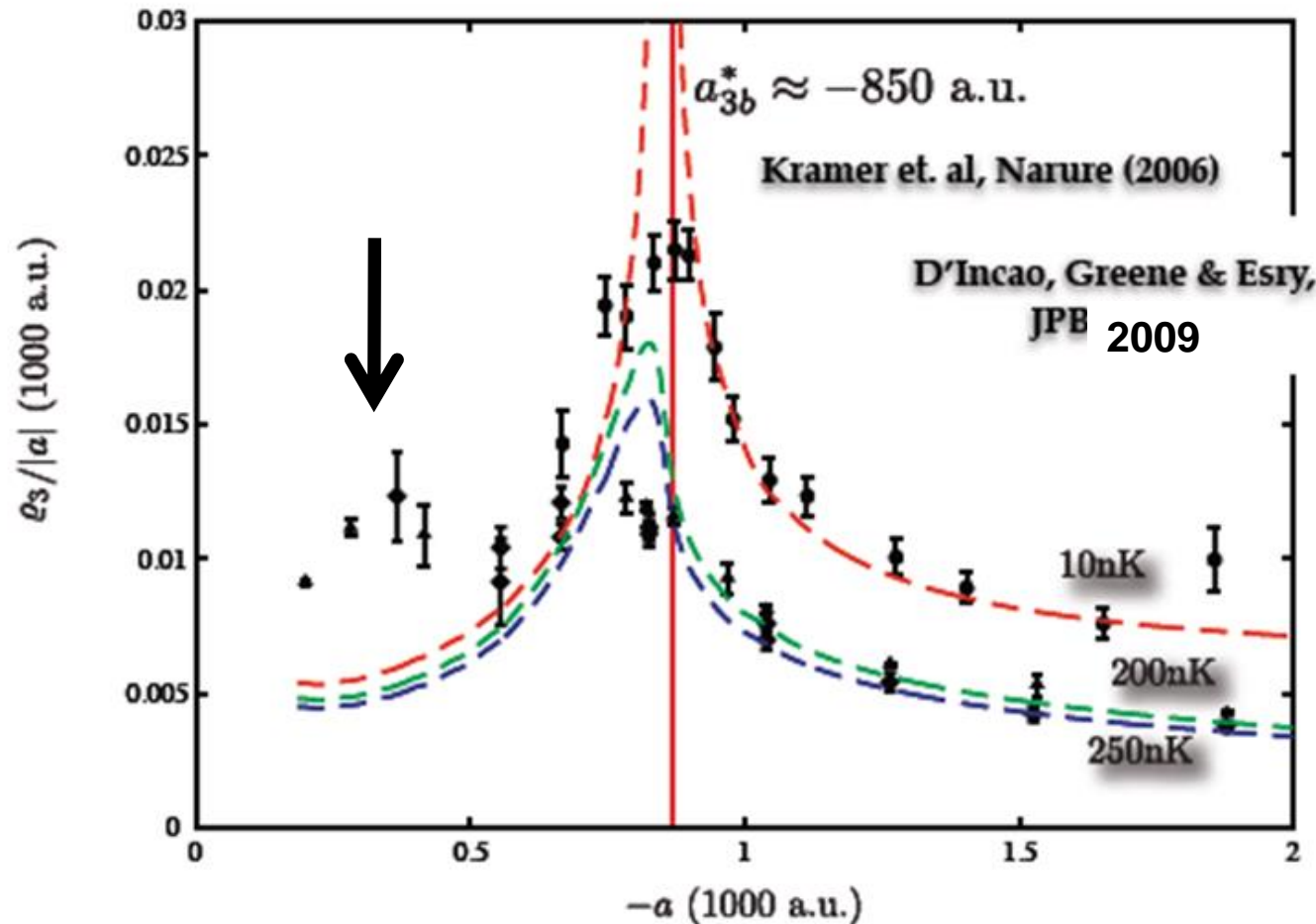
# Revisiting the 2006 Grimm group experiment that was the first to see 3-body Efimov states

NATURE PHYSICS | VOL 5 | JUNE 2009 | p.417

## Signatures of universal four-body phenomena and their relation to the Efimov effect

von Stecher,  
D’Incao, CHG

Considering **only** three-body recombination ...



But before we could actually calculate the rate of 4-body recombination in an ultracold gas, we had to develop some scattering theory:

PRL 103, 153201 (2009)

## A general theoretical description of N-body recombination

N. P. Mehta,<sup>1,2</sup> Seth T. Rittenhouse,<sup>1</sup> J. P. D’Incao,<sup>1</sup> J. von Stecher,<sup>1</sup> and Chris H. Greene<sup>1</sup>

<sup>1</sup>*Department of Physics and JILA, University of Colorado, Boulder, CO 80309*

<sup>2</sup>*Grinnell College, Department of Physics, Grinnell, IA 50112\**

(Dated: March 24, 2009)

We present a formula for the cross section and event rate constant describing recombination of  $N$  particles in terms of general  $S$ -matrix elements. Our result immediately yields the generalized Wigner threshold scaling for the recombination of  $N$  bosons. We find that four-boson recombination is resonantly enhanced by the presence of metastable states in the entrance channel. Hence, recombination into a trimer-atom channel could be an effective mechanism for the formation of Efimov trimers.

And here it is, **THE FORMULA** for N-body recombination, i.e. for the process:  $A+A+A+\dots+..A \rightarrow A_{N-1}+A$  or  $A_{N-2}+A+A +\dots$ etc.

$$K_N^{0+} = \frac{2\pi\hbar}{\mu_N} N! \left( \frac{2\pi}{k} \right)^{(3N-5)} \frac{\Gamma((3N-3)/2)}{2\pi^{(3N-3)/2}} \left| S_{f0}^{0+} \right|^2$$

In  $d$  dimensions, the wave function at large  $R$  behaves as

$$\Psi^I \rightarrow e^{i\hat{k}\cdot\hat{R}} + f(\hat{k}, \hat{k}') \frac{e^{ikR}}{R^{(d-1)/2}}. \quad (1)$$

**Some formal work to generalize scattering theory to  $d$ -dimensions**

Equivalently, an expansion in hyperspherical harmonics is written in terms of unknown coefficients  $A_{\lambda\mu}$ :

$$\Psi^{II} = \sum_{\lambda,\mu} A_{\lambda\mu} Y_{\lambda\mu}(\hat{R}) [j_{\lambda}^d(kR) \cos\delta_{\lambda} - n_{\lambda}^d(kR) \sin\delta_{\lambda}]. \quad (2)$$

Here,  $Y_{\lambda\mu}$  are hyperspherical harmonics (solutions to the free-space angular equation  $[\Lambda^2 - \lambda(\lambda + d - 2)]Y_{\lambda\mu} = 0$ , where  $\Lambda^2$  is the grand angular momentum operator [14]) and  $j_{\lambda}^d$  ( $n_{\lambda}^d$ ) are hyperspherical Bessel (Neumann) functions [14].

### Scattering amplitude, purely hyperradial potential, phaseshifts

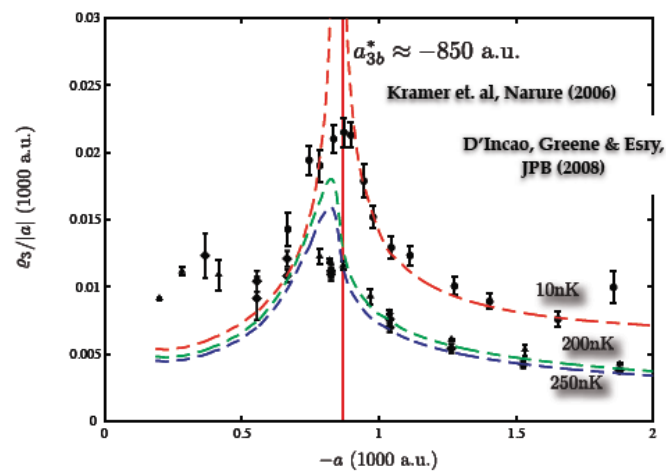
$$f(\hat{k}, \hat{k}') = \left(\frac{2\pi}{k}\right)^{(d-1)/2} \sum_{\lambda\mu} i^{\lambda} e^{-i(d/2-1+\lambda)\pi/2-i\pi/4} Y_{\lambda\mu}^*(\hat{k}) \times Y_{\lambda\mu}(\hat{k}') (e^{2i\delta_{\lambda}} - 1).$$

$$\sigma_{fi}^{\text{indist}(J^{\Pi})} = N_p \left(\frac{2\pi}{k_i}\right)^{d-1} \frac{1}{\Omega(d)} \sum_i (2J + 1) |S_{fi}^{J^{\Pi}} - \delta_{fi}|^2.$$

where  $\Omega(d) = 2\pi^{d/2}/\Gamma(d/2)$  is the total solid angle in  $d$  dimensions [14]. This last expression is immediately

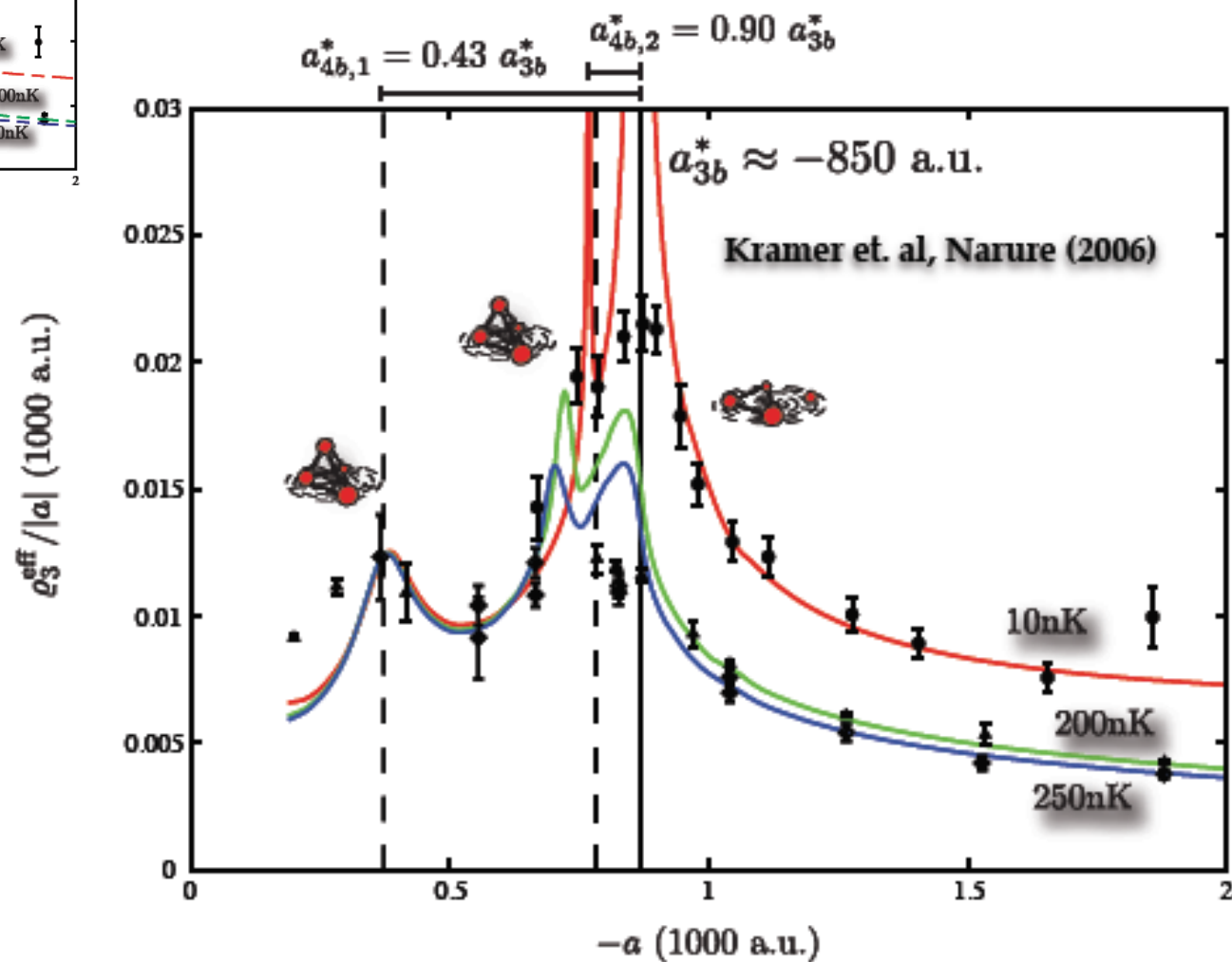


Considering **only** three-body recombination ...



Considering **three-** and **four-**body recombination ...

$$K_3^{\text{eff}}(a, t) = K_3(a) + n(t)K_4(a)$$



# Evidence for Universal Four-Body States Tied to an Efimov Trimer

F. Ferlaino,<sup>1</sup> S. Knoop,<sup>1</sup> M. Berninger,<sup>1</sup> W. Harm,<sup>1</sup> J. P. D’Incao,<sup>2,3</sup> H.-C. Nägerl,<sup>1</sup> and R. Grimm<sup>1,2</sup>

PRL 102, 140401 (2009)

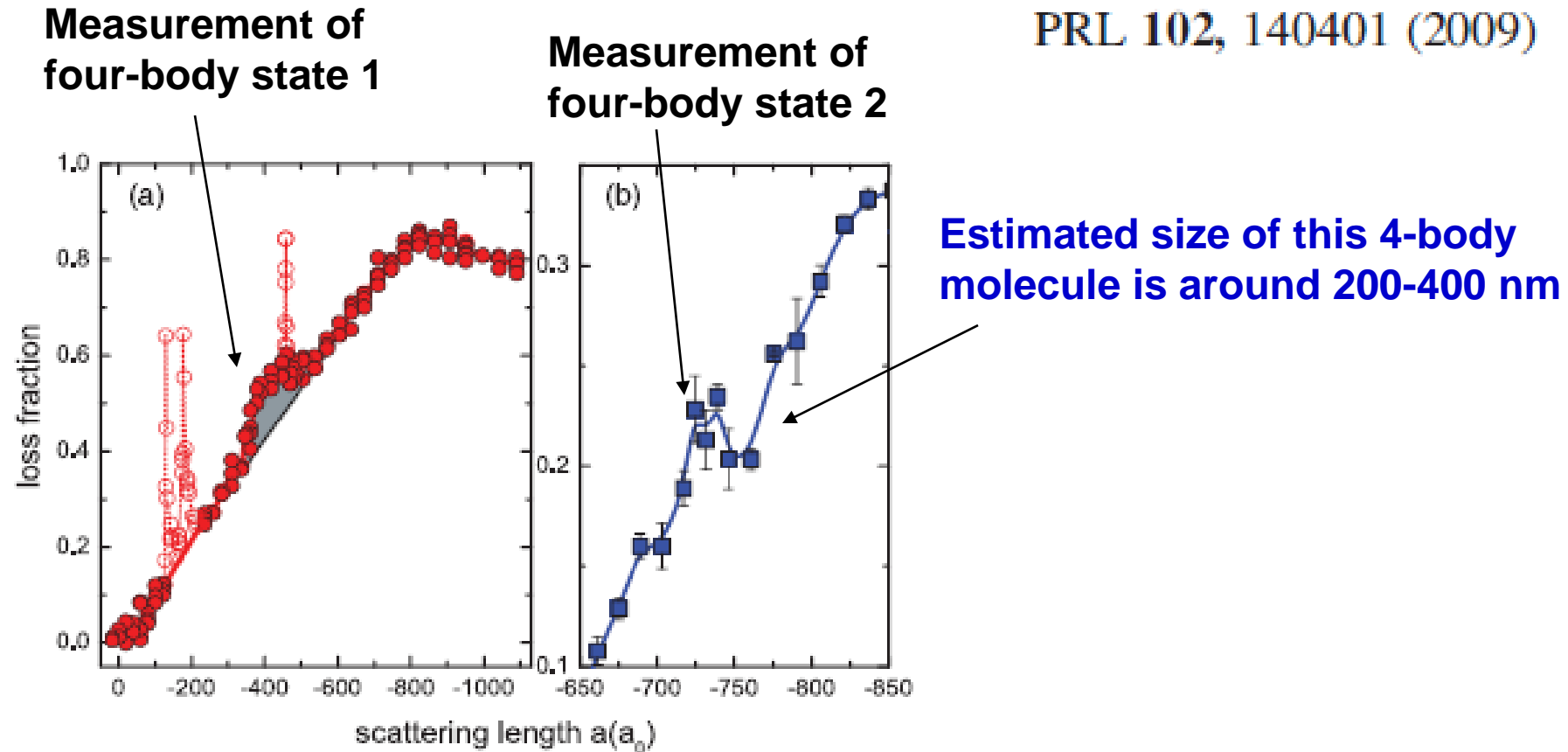


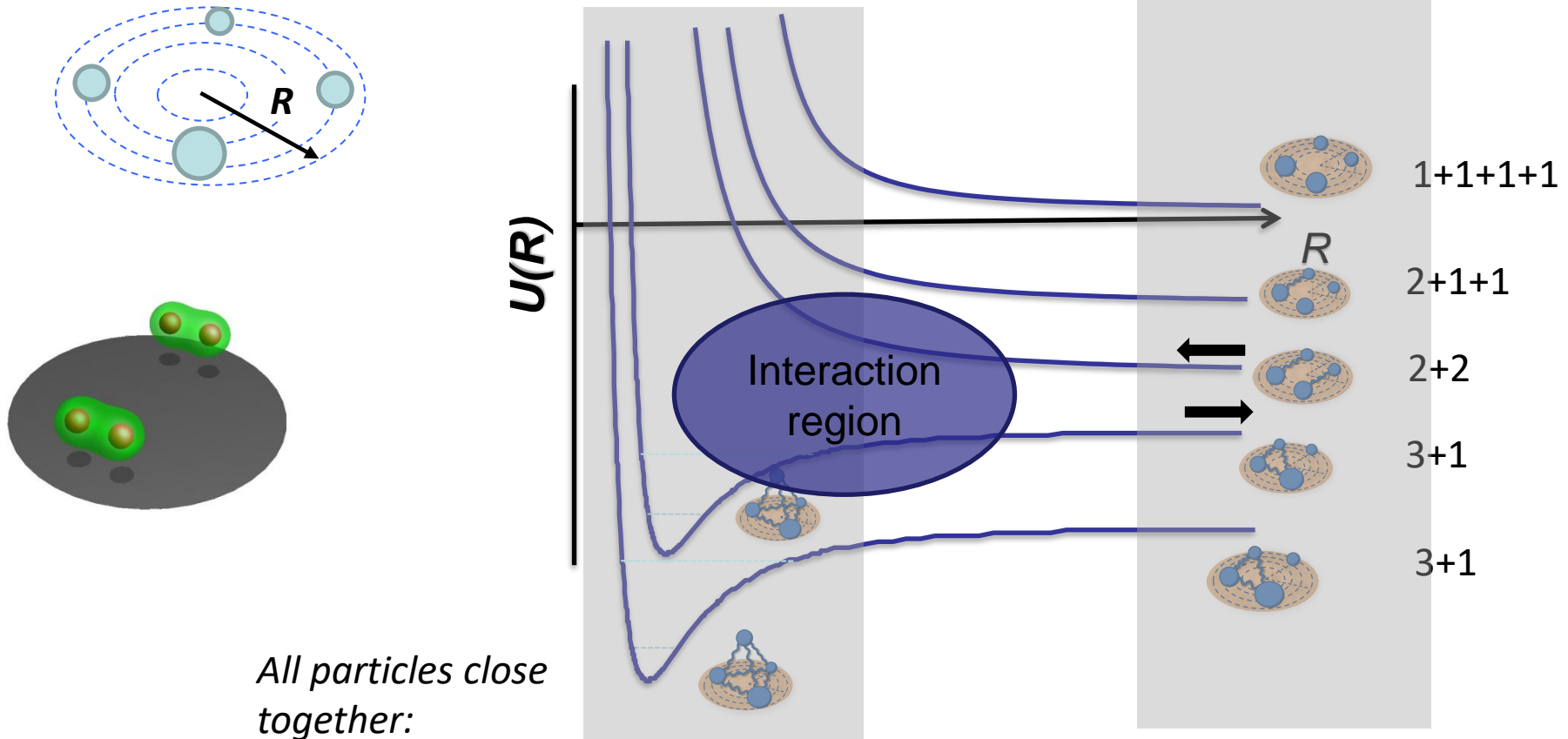
FIG. 2 (color online). Recombination losses in an ultracold sample of Cs atoms. (a) Loss fraction for a 50-nK sample after a storage time of 250 ms. Here we present all individual measurements to give an impression of the scatter of our data. The broad maximum at about  $-870a_0$  is caused by a triatomic Efimov resonance [7] and the shaded area highlights the resonant loss enhancement that we attribute to the four-body state Tetra1. The



# Hyperspherical Picture

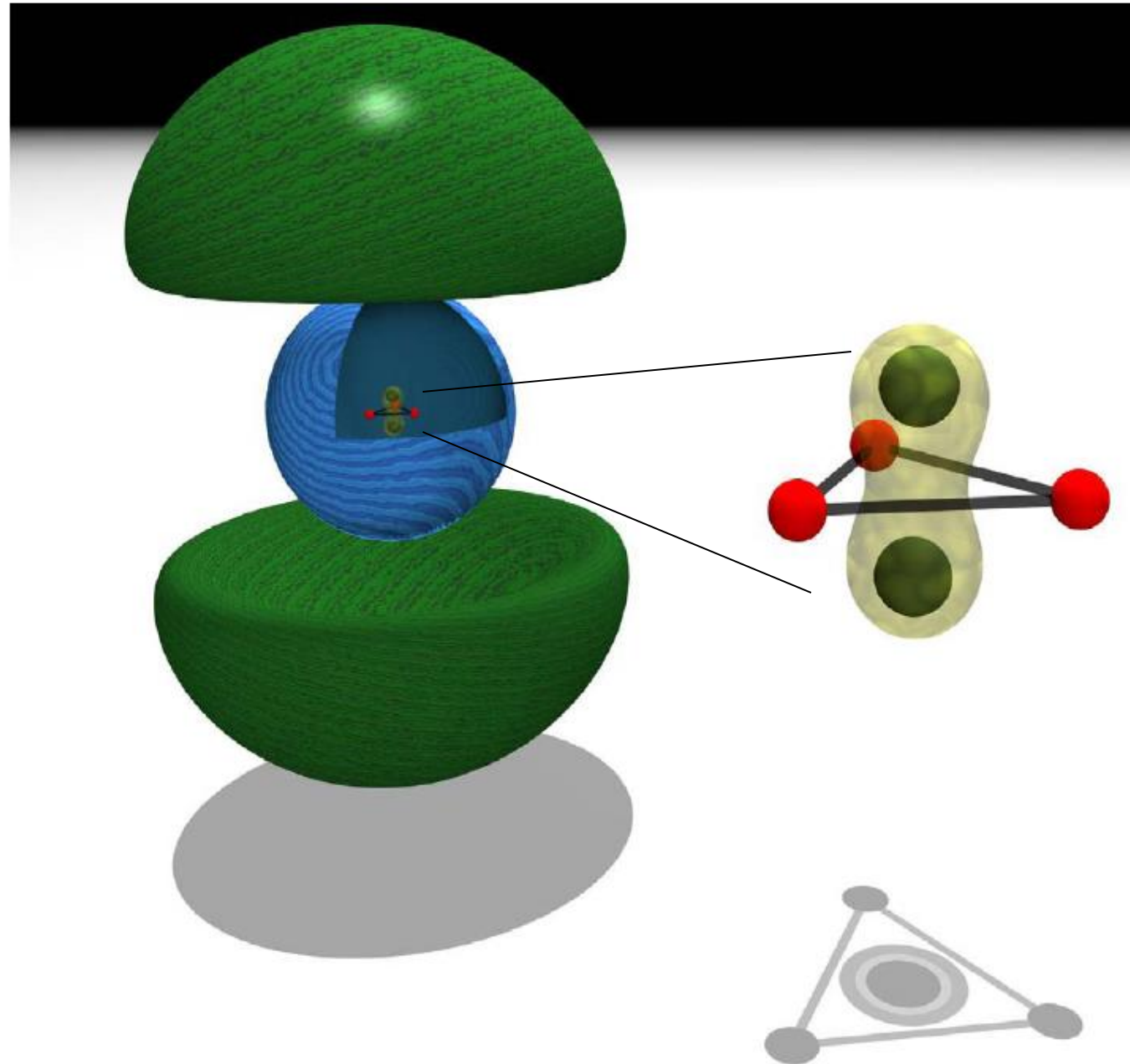
... think Born Oppenheimer

Fragmentation thresholds



All particles close together:  
Bound and quasi-bound states

Bird's-eye view of the higher-energy tetramer, very weakly bound



# Conclusions

**The tools of scattering theory can be applied to ultracold atomic systems, as well as to atomic and molecular Rydberg states**

**Multichannel quantum defect theory extends the idea of a scattering or reaction matrix by including CLOSED channels, which can give smooth and weak energy dependent quantities that characterize a very rich spectrum with a huge number of resonances**

**The time delay matrix can be used to study the decay probabilities of a resonance into the alternative possible decay channels**

**For collisions of 3- or more bodies in the N-body continuum, the adiabatic hyperspherical representation gives a set of potential energy curves that can be used to interpret the resonance properties qualitatively and even semi-quantitatively**